The authors are grateful to the anonymous referee #3 for his/her constructive comments and suggestions. Here, we present the response for each of the comments. The revised manuscript and supplement with tracked changes can be found at the end of the document.

1. PMF analysis-

- **PMF was performed separately on each season. Was there enough data in during 2020 to draw meaningful conclusions? It is difficult to tell the duration of measurements from figure 1.**

Authors' response: We presented 20 days data (464 data points) for the spring season in 2020 (April 15 - May 4). Due to the instruments failure, we could not continue the measurements for a longer period. Still, PMF model analysis on 464 hourly data points is enough to draw a meaningful conclusion.

- **Do the PMF results indicate that there is seasonality in source sector emissions, or are the fingerprints consistent?**

Authors' response: Yes, the PMF results indicate that there is seasonality in source sector emissions, for instance, (i) contribution from gasoline evaporation was much higher in summer than those in autumn and spring (ii) biogenic source was clearly distinguished in summer (due to high emission), but mixed with other sources during the rest of the seasons.

- **Why was an 8 factor solution chosen (v. 7 v. 6 factors, etc)?**

Authors' response: The reason for choosing 7 to 8-factor solution has been mentioned in the material and methods (section 2.2) of the revised manuscript (added at the end of this document).

- **The supplemental figures are difficult to read due to the number of species included in the figure. It should be noted which axis should be read with each dataset.**

Authors' response: Both the issues have been solved in the revised manuscript.

- **As noted by reviewer 2, the results are odd (e.g., biogenic isopentane; propane from**

solvents). The revised and trimmed-down PMF submitted in response to the reviewer still has these oddities.

Authors' response: It has been solved in the revised manuscript added below. For instance, isopentane is assigned to gasoline evaporation and propane is assigned to LPG/NG usages sources.

2. PSCF analysis-

• I do not think this method is ubiquitous enough to merit the brevity of explanation. For example, what do the colors mean in figure 5? What does the impact of a 24 v. 48 v. 72 h back-trajectory have on the analysis? Does this assume that VOCs have the same lifetime as the back-trajectory?

Authors' response: PSCF has been widely used to determine potential source areas of particulate pollutants, and in recent years, it has been also used to determine the potential source areas of VOCs (Hao et al., 2019; Ming et al., 2017; Sun et al., 2015; Song et al., 2018; Hui et al., 2019). The PSCF value itself is a probability (from 0 to 1) indicating the probability of being a possible source of a pollutant (e.g. colorbar in Figure 5). This probability is calculated by dividing the number of trajectories with a high air pollutant concentration (higher than the mean TVOCs concentration in our case) by the total number of trajectories at the receptor. Areas in Figure 5 with higher PSCF values indicate that the corresponding region is a potential source region of severe VOC pollution. We generally choose backward trajectories of different duration depending on the studied species, for example, if it is an inert pollutant such as Black Carbon, a backward trajectory of 120h or longer will be chosen. The biggest difference between 24h vs 48h vs 72h analysis is that we assume different atmospheric lifetimes of the pollutants, so that the potential source area obtained is also different, e.g., the range of 72h is larger and the high probability range (high PSCF value) is larger too, but if the pollutants themselves are not able to remain for 72h, there will be some bias in the estimation of the potential source area.

• It is not clear what useful/new information is derived from this analysis. The main results of this analysis (line 428-430) seems to be that the VOCs measured at the site

come primarily come from industries located near the site. Would there be a reason to think otherwise?

Authors' response: Long-distance transport of VOC pollution to the receptor site is not uncommon (Derstroff et al., 2017; Patokoski et al., 2015). So, it is not always the case that the VOC should come to the measurement site from the nearby areas.

3. OFP/EKMA/RIR

• Discussion of wintertime OFP seems unusual, as photochemical ozone production in the winter is not a primary concern.

Authors' response: The OFP analysis has already been removed following the suggestion of referee #2.

• There are not enough details in the description of the F0AM model. For example: Which VOCs were constrained (not all are in MCM)?

Authors' response: More information has been added in the methods, and the list of constrained VOCs has been added in Table S1.

Other comments-

• I find the title "High Contributions of Halohydrocarbon and Aromatic Compounds to Emissions and Chemistry of Atmospheric VOCs in Industrial Area" to be misleading. Halocarbons do not contribute significantly to either SOA or ozone chemistry. Neither halocarbons nor aromatics dominate calculated OFP in the summer (Figure 5).

Authors' response: The title has been modified in the revised version.

• It seems a major conclusion (line 431) is that industries and vehicles should have the most priority in reducing emissions. Nearly all anthropogenic VOCs in this area could

be classified as industry/vehicles, so this conclusion seems too vague to be meaningful. Is it a new finding?

Authors' response: This part has been modified in the revised manuscript. According to the revised PMF model analysis vehicle-related emissions were the major VOC sources in the industry affected area.

- **It is unusual to see the notation KOH (typically lowercase/supscripts are for kinetics, uppercase for equilibrium reactions).**

Authors' response: Amended.

- **There are no units in supplemental tables.**

Authors' response: Units have been added in the supplemental tables.

- **It is not clear how to interpret numbers given in lines 272 (e.g., 0.9-2 (1.4 +/- 0.3))**

Authors' response: It was the range and mean value of toluene to benzene ratio in ppbv/ppbv unit. The toluene to benzene ratio analysis section has already been removed following the suggestion of referee #2.

References

Derstroff, B., Hüser, I., Bourtsoukidis, E., Crowley, J. N., Fischer, H., Gromov, S., … Williams, J. (2017). Volatile organic compounds (VOCs) in photochemically aged air from the eastern and western Mediterranean. *Atmospheric Chemistry and Physics*, *17*(15), 9547–9566. https://doi.org/10.5194/acp-17-9547-2017

Hao, T., Cai, Z., Chen, S., Han, S., Yao, Q., & Fan, W. (2019). Transport pathways and potential source regions of PM2.5 on the west coast of Bohai Bay during 2009-2018. *Atmosphere*, *10*(6). https://doi.org/10.3390/atmos10060345

Hui, L., Liu, X., Tan, Q., Feng, M., An, J., Qu, Y., … Cheng, N. (2019). VOC characteristics, sources and contributions to SOA formation during haze events in Wuhan, Central China. *Science of the Total Environment*, *650*, 2624–2639. https://doi.org/10.1016/j.scitotenv.2018.10.029

Ming, L., Jin, L., Li, J., Fu, P., Yang, W., Liu, D., … Li, X. (2017). PM2.5 in the Yangtze River Delta, China: Chemical compositions, seasonal variations, and regional pollution events. *Environmental Pollution*, *223*, 200–212. https://doi.org/10.1016/j.envpol.2017.01.013

Patokoski, J., Ruuskanen, T. M., Kajos, M. K., Taipale, R., Rantala, P., Aalto, J., … Rinne, J. (2015). Sources of long-lived atmospheric VOCs at the rural boreal forest site, SMEAR II. *Atmospheric Chemistry and Physics*, *15*(23), 13413–13432. https://doi.org/10.5194/acp-15-13413-2015

Song, M., Tan, Q., Feng, M., Qu, Y., Liu, X., An, J., & Zhang, Y. (2018). Source Apportionment and Secondary Transformation of Atmospheric Nonmethane Hydrocarbons in Chengdu, Southwest China. *Journal of Geophysical Research: Atmospheres*, *123*(17), 9741–9763. https://doi.org/10.1029/2018JD028479

Sun, Y. L., Wang, Z. F., Du, W., Zhang, Q., Wang, Q. Q., Fu, P. Q., … Worsnop, D. R. (2015). Long-term real-time measurements of aerosol particle composition in Beijing, China: Seasonal variations, meteorological effects, and source analysis. *Atmospheric Chemistry and Physics*, *15*(17), 10149–10165. https://doi.org/10.5194/acp-15-10149-2015

Measurement report: High Contributions of Halocarbon and Aromatic Compounds to ~~Emissions and Chemistry of~~ Atmospheric VOCs in Industrial Area

Ahsan Mozaffar [1,2,3], Yan-Lin Zhang [1,2,3*], Yu-Chi Lin[1,2,3], Feng Xie [1,2,3], Mei-Yi Fan [1,2,3], and Fang Cao [1,2,3]

[1]Yale-NUIST Center on Atmospheric Environment, International Joint Laboratory on Climate and Environment Change, Nanjing University of Information Science and Technology, Nanjing, 210044, China.

[2]Key Laboratory Meteorological Disaster; Ministry of Education & Collaborative Innovation Center on Forecast and Evaluation of Meteorological Disaster, Nanjing University of Information Science and Technology, Nanjing, 210044, China.

[3]Jiangsu Provincial Key Laboratory of Agricultural Meteorology, College of Applied Meteorology, Nanjing University of Information Science & Technology, Nanjing 210044, China.

Correspondence to: Yan-Lin Zhang (dryanlinzhang@outlook.com)

Abstract. Volatile organic compounds (VOCs) are key components for tropospheric chemistry and air quality. We investigated ambient VOCs in an industrial area in Nanjing, China for about 1 month in winter, spring, and summer and 3 months in autumn ~~from~~ between July 2018 ~~to~~ and May 2020. The total VOCs (TVOCs) concentration was 59.8±28.6 ppbv during the investigation period. About twice TVOCs concentrations were observed in autumn (83±20 ppbv) and winter (77.5±16.8 ppbv) seasons compared to those in spring (39.6±13.1 ppbv) and summer (38.8±10.2 ppbv). ~~Unlike~~ In previous studies in Nanjing, oxygenated-VOCs (OVOCs) and halocarbons were not measured, ~~the observed TVOCs was about 1.5 and 3 times higher than those previously reported in the same study area and a nonindustrial suburban area in Nanjing, respectively~~ the current TVOCs concentration without halocarbons and OVOCs was similar to the previous investigation in the same study area, however, 2 folds higher than the one reported in the nonindustrial suburban area in Nanjing. Observed TVOCs concentration~~s~~ ~~were~~ was similar to ~~those~~ the one in the metropolitan city Beijing, ~~and~~ but, 1.3 fold smaller than the one reported in Shanghai.~~,~~ Observed TVOCs concentration was similar to those in Lanzhou, Chengdu, Tokyo, and Xi'an, however, it was about 1.5-~~3~~ 1.7 folds higher than those in ~~Lanzhou,~~ Wuhan, Tianjin, and Ningbo~~, Chengdu, London, Los Angeles, and Tokyo~~. Due to the industrial influence,

halocarbons (14.3±7.3 ppbv, 24%) VOC-group was the second largest contributor to the TVOCs after alkanes (21±7 ppbv, 35%), which is in contrast with the previous studies in Nanjing and also in almost other regions in China. Relatively high proportions of helohydrocarbons and aromatics were observed in autumn (25.7 and 19.3%, respectively) and winter (25.8 and 17.6%, respectively) compared to those in summer (20.4 and 11.8%, respectively) and spring (20.3 and 13.6%, respectively). According to the potential source contribution function (PSCF), short-distance transports from the surrounding industrial areas and cities were the main reason for high VOC concentration in the study area. According to positive matrix factorization (PMF) model results, ~~industry related sources (23-47%) followed by~~ vehicle-related emissions (~~24~~33-~~34~~48%) contributed the major portion to the ambient VOC concentrations. ~~Whereas aromatics~~ Aromatics followed by alkenes were the top contributors to the loss rate of OH radicals (L_{OH}) (37 and 32%, respectively)~~, alkenes followed by aromatics contributed most to the ozone formation potential (OFP) (39 and 28%, respectively)~~. ~~Besides, the aromatics VOC-group was also the major contributor to the secondary organic aerosol potential (SOAP) (97%).~~ According to the empirical kinetic modelling approach (EKMA) and relative incremental reactivity (RIR) analysis in assistance with a photochemical box model, the study area was in the VOC-sensitive regime for ozone (O_3) formation during all the measurements seasons. Therefore, mainly alkenes and aromatics emissions chiefly from ~~industries and~~ automobiles should be reduced to decrease the secondary air pollution formation in the study area.

1 Introduction

Air pollution characterized by severe ozone (O_3) and haze pollution is a big problem in urban and industrial areas in China (He et al., 2019; Hui et al., 2018; Tan et al., 2018; Jia et al., 2016; Feng et al., 2016; Hui et al., 2019). In recent years, O_3 concentration above the national standard, and severe haze events are frequently reported (He et al., 2019; Hui et al., 2019; Sheng et al., 2018; Feng et al., 2016; Tan et al., 2018; Jia et al., 2016). As a precursor of O_3 and secondary organic aerosol (SOA), volatile organic compounds (VOCs) are largely responsible for the severe air pollution in China (Song et al., 2018; Hui et al., 2019; Hui et al., 2018; He et al., 2019). Unfortunately, anthropogenic VOC emissions have been increasing over the last 2 decades in China and it is expected to do so in the future (Mozaffar & Zhang, 2020, and references therein).

Atmospheric VOC has plenty of sources; it can be emitted from various anthropogenic and biogenic sources. Besides, it can also be formed in the atmosphere. Anthropogenic VOC sources mainly include industrial emission, vehicle exhaust, solvent usages, biomass burning, and fuel evaporation. On the other hand, vegetation is the main biogenic sources of VOC. In developed areas in China, vehicle exhaust and industrial emission are the 2 major VOC sources (He et al., 2019; Hui et al., 2018; Hui et al., 2019; Mo et al., 2017; Song et al., 2018; An et al., 2014; Mozaffar & Zhang, 2020). Whereas vehicle-related sources are more dominant in the North China Plain (NCP), Central China (CC), and Pearl River Delta region (PRD), industry-related sources are more influential in the Yangtze River Delta (YRD) area (Zhang et al., 2017; Meng et al., 2015; Sun et al., 2019; He et al., 2019; Zhang et al., 2018; An et al., 2017; Mozaffar & Zhang, 2020; Shao et al., 2016). Alkanes, Alkenes, aromatics, oxygenated-VOCs (OVOCs), and halocarbons are the most common VOC-groups in the atmosphere (Hui et al., 2019; Hung-Lung et al., 2007; Song et al., 2018; Tiwari et al., 2010; He et al., 2019; Na et al., 2001; Hui et al., 2018). VOC concentration and composition changes depending on seasons, for example, the contribution from biogenic and solvent utilization increases in summer, and contribution from combustion sources increases in winter (Mo et al., 2017; Song et al., 2018; An et al., 2014). The chemical reactivity of VOC depends on its chemical composition, for instance, alkenes and aromatics are generally more reactive than alkanes (Carter, 2010). To understand the chemical reactivity ~~and secondary product formation ability~~ of VOCs, analysis of OH radical loss rate (L_{OH})~~, ozone formation potential (OFP), and secondary organic aerosol potential (SOAP) are~~ is commonly used (~~Song et al., 2018; He et al., 2019;~~ Hui et al., 2018~~); Hui et al., 2019)~~.

Industries are an important source of VOC, and different reactive and hazardous VOCs emissions from industries are already reported in different areas on earth (Zhang et al., 2018; Na et al., 2001; Hung-Lung et al., 2007; Yan et al. 2016; Tiwari et al., 2010; Shi et al., 2015; Zhang et al., 2018b). For instance, Zhang et al. (2018) reported a high concentration of alkanes (82%) and lifetime cancer risk of different aromatics and halocarbons in a petroleum refinery in Guangzhou, China. A high concentration of OVOCs (63%) was observed in an industrial area in Ulsan, Korea (Na et al., 2001). Hung-Lung et al.(2007) mentioned a high concentration of aromatics in an industrial area in Taiwan. A high concentration of halocarbons (49%) was observed in an iron smelt plant in Liaoning, China (Shi et al., 2015). Zhang et al. (2018) mentioned a high concentration of alkanes (42%) and aromatics (20%) in a petrochemical and

other industries affected area in Shanghai, China. High concentrations of aliphatic and aromatics were observed in a petrochemical industrial area in Yokohama, Japan (Tiwari et al., 2010). Therefore, VOC composition varied among the industries/industrial areas in different regions. Mostly short-term investigations were performed to characterize the VOCs in industry-affected areas. In the current study, we carried out a comprehensive investigation on VOC in an industrial area in Nanjing for about 1 month in winter, spring, and summer and 3 months in autumn between July 2018 and May 2020. Nanjing is located in the YRD region which is mainly affected by industrial emissions. Several VOC investigations have already been performed in the Nanjing industrial area but OVOCs and halocarbons were not measured in those studies (An et al., 2017; An et al., 2014). However, OVOCs and halocarbons are already mentioned as one of the highest concentrated VOC-groups in other industrial regions (Na et al., 2001; Shi et al., 2015). In the current study area, a high concentration of alkanes (45%) and alkenes (25%) were observed in a previous investigation (An et al., 2014). Besides the incomplete VOC measurements, O_3 formation sensitivity to its precursors was not investigated properly using a photochemical box model in Nanjing. Moreover, source apportionment of VOCs was not conducted for different seasons of a year.

In the current study, we report the variations in concentrations and compositions of VOC during the observation period. We present the possible source areas and potential sources of VOC based on potential source contribution function (PSCF) and positive matrix factorization (PMF) model analysis. We also present the contributions of different sources to ambient VOC during the measurement period. We report the chemical reactivity ~~and secondary product formation capacity~~ of the VOC using L_{OH}~~, OFP, and SOAP analysis~~. We also present the sensitivity analysis of O_3 formation using empirical kinetic modelling approach (EKMA) and relative incremental reactivity (RIR) analysis. Therefore, this study provides valuable information to the scientific community and policymakers.

2 Material and Methods

2.1 Sampling Site Description, Gases Analysis, and Meteorology Data

Field measurements were carried out for about 1 month in winter, spring, and summer and 3 months in autumn ~~from~~ between July 2018 ~~to~~ and May 2020 at Nanjing University of Information Science and Technology (32.1°N, 118.4°E), which is located in an industrial area in Nanjing, China. The sampling site was on the rooftop of a building (~20 m). The sampling site is surrounded by different chemical and petrochemical industries, steel plants, gas stations, high traffic roads, and residential areas. A detailed description of the sampling site can be found elsewhere (Mozaffar et al., 2020).

We analysed ambient air VOCs using an online GC-FID/MS instrument (AC-GCMS 1000, Guangzhou Hexin Instrument Co., Ltd., China). FID detector analysed C2-C5 VOCs and MS analysed C6-C12 VOCs. The instrument analysed one sample at every hour. During the investigation period, we inspected and calibrated the instrument regularly to ensure the accuracy of the data. We monitored the O_3 concentrations using a 49i O_3 analyser (Thermo Fisher Scientific Inc., USA), NO, NO_2 and NOx concentrations were measured using a 42i NO-NO_2-NOx analyser (Thermo Fisher Scientific Inc., USA), SO_2 concentrations were followed using a 43i SO_2 analyser (Thermo Fisher Scientific Inc., USA), and CO concentrations were measured using a 48i CO analyser (Thermo Fisher Scientific Inc., USA). We also measured temperature and relative humidity, wind speed, wind direction, and solar radiation by HMP155 (Vaisala, Finland), 010C (Met One Instruments, Inc., USA), 020CC (Met One Instruments, Inc., USA), and CNR4 (Kipp & Zonen, The Netherlands) analysers, respectively. A detailed description of the instrumentation, sampling procedure, analysis, quality control, and calibration procedure can be found elsewhere (Mozaffar et al., 2020).

2.2 Positive Matrix Factorization (PMF) model and Potential Source Contribution Function (PSCF)

We used the positive matrix factorization (PMF) model (US Environmental Protection Agency, USEPA, version 5.0) for the source apportionments of VOCs. A detailed description of the model can be found elsewhere (Hui et al., 2019; Song~~, Tan, Feng, Qu, Liu,~~ et al., 2018). In this study, we used ~~6~~20 potential VOC tracers (Fig. S1 - S4) in the PMF model to analyse the VOC sources for different seasons. The error fraction was set to 20% for the sample data uncertainty

estimation. We explored the PMF factor number from 4-8 to determine the optimal number of sources. Finally, we decided to choose a~~n~~ 7 to 8-factor solution ~~(Q_{true}/Q_{robust} = ~1.0)~~for different seasons as Q_{true}/Q_{robust} was ~1.0, $Q_{true}/Q_{expected}$ was ranging from 0.99-1.45 (Hui et al., 2019), and strong correlations (0.7-0.8) were observed between the concentrations extracted from the model and the observed concentrations of each compounds (He et al., 2019).

We used the potential source contribution function (PSCF) to locate possible source areas of VOCs for different seasons during the investigation period. We used Zefir analysis software to do the PSCF analysis and the Hysplit4 model to cluster the backward trajectories (Petit et al., 2017). Backward trajectories in the sampling site were estimated using the data provided by the National Centers for Environmental Prediction (ftp://arlftp.arlhq.noaa.gov/pub/archives/gdas1). We estimated ~~24~~ 72 hr backward trajectories 24 times a day arriving at 500 m above the ground surface using the hysplit4 model. For the PSCF analysis, we divided the geographic region covered by the back trajectories into an array of 0. 1° × 0. 1° grid cells and used the mean TVOCs concentration as the VOC reference value. More details about the PSCF analysis can be found in previous studies (Chen et al., 2018).

2.3 OH radical loss rate (L_{OH})~~, Ozone formation potential (OFP), and Secondary organic aerosol potential (SOAP)~~

To evaluate the daytime photochemistry of VOCs, we estimated their OH radical loss rate (L_{OH}). The following equation was used to estimate the L_{OH} (s^{-1}) (Zhang et al., 2020).

$$L_{OH} = [VOC]_i \times K_{OHi} \quad (1)$$

Where $[VOC]_i$ is the concentration of VOC species i (molecule cm^{-3}), K_{OHi} (cm^3 $molecule^{-1}$ s^{-1}) is the reaction rate constant of i VOC with OH radical. The K_{OH} values for the VOCs are collected from Carter (2010) (Table S1).

~~The Ozone formation potential (OFP) of the VOCs is their maximum contribution to the O_3 formation (Hui et al., 2018a). The OFP (ppbv) of the VOCs was estimated using the following equation.~~

~~$OFP = [VOC]_i \times MIR_i$~~

~~(2)~~

~~Where MIR_i is the maximum incremental reactivity of the i VOC. The MIR values for the VOCs are also collected from Carter (2010) (Table S1).~~

~~The contribution of VOCs to the formation of secondary organic aerosol is estimated by secondary organic aerosol potential (SOAP) (Song et al., 2018). We estimated the SOAP (ppbv) of VOCs using the following equation.~~

~~$$SOAP = [VOC]_i \times SOAP_i^p \quad (3)$$~~

~~Where $SOAP_i^p$ is the SOA formation potential of the i VOC on a mass basis relative to toluene (Derwent et al., 2010). In this study, the $SOAP^p$ factors of the VOCs are collected from Derwent et al.(2010) (Table S1).~~

2.4 Empirical Kinetic Modelling Approach (EKMA) and Relative Incremental Reactivity (RIR)

The empirical kinetic modelling approach (EKMA) is a well-known procedure to develop the O_3 formation reduction strategy by testing the relationship between ambient O_3 and its precursors (He et al., 2019; Hui et al., 2018; Vermeuel et al., 2019; Tan et al., 2018). In this study, we used the Framework for 0-D Atmospheric Model (F0AM v 3.2, Wolfe et al., 2016), a photochemical box model run by Master Chemical Mechanism (MCM) v3.2 chemistry (Jenkin et al., 1997; 2003, 2015; Saunders et al., 2003), to get the data for the EKMA isopleth. The FOAM-MCM box model can simulate 16940 reactions of 5733 chemical species. The box model was run using the VOCs and gas concentrations and the meteorological data as input. 61 VOCs were constrained in the model as all the observed VOC species reactions are not included in MCM. These constrained VOCs are listed in Table S1. To generate the O_3 isopleth from the model simulated data, a total of 121 reduction scenarios (11 NOx ×11 VOC) were simulated and the maximum O_3 produced in each scenario was saved.

The O_3 formation sensitivity to its precursors' concentrations can also be assessed by the relative incremental reactivity (RIR, Cardelino & Chameides, 1995). We also utilized the FOAM-MCM box model data to estimate the RIR. The RIR is simply defined as the percentage change in O_3 formation per percentage change in precursor's concentration. In this study, we reduced the precursor's concentration by 10% for the RIR estimation. The RIR was estimated using the following equation.

$$RIR\ (X) = \frac{[P_{O_3}(X) - P_{O_3}(X-\Delta X)]/P_{O_3}(X)}{[\Delta X]/[X]} \quad (2)$$

Where [X] is the observed concentration of a precursor X, [ΔX] is the changes in the concentration of X. $P_{O3}(X)$ and $P_{O3}(X- \Delta X)$ are the simulated net O_3 production with the observed and the reduced concentration of the precursor X, respectively.

3 Results and discussion

3.1 Overview of the metrological conditions and air pollutants concentrations

The time series of the hourly inorganic air pollutants, meteorological parameters, and TVOC concentrations estimated with all the measured VOCs and without halocarbons are shown in Fig. 1. The discontinuity of the time series data is due to the failure of the instruments. The measured data from July to August 2018, September to November 2018, December 2018 to January 2019, and April to May 2020 are termed as summer, autumn, winter, and springtime data, respectively. Overall, the observed temperature and solar radiation gradually decreased from summer to winter and increased back to the summertime level in spring. The temperature ranged between -5.7 and 41.4 °C during the measurement period. The relative humidity values varied from 18 to 100% and high values were generally observed in winter and autumn. During the observation period, wind speed ranged between 0.1 and 7.5 ms^{-1}. Wind prevailed at the sampling site from many directions during the measurement periods; more details about the wind direction will be discussed in Sect.3.3.2. The O_3 and NOx concentrations varied from 2 to 160 ppbv and 0.4 to 90 ppbv, respectively. Whereas high O_3 concentrations (>80 ppbv) were observed in summer and spring, high NOx concentrations were measured in winter and at the end of autumn. The CO and SO_2 concentrations ranged from 83 to 3398 ppbv and 0.5 to 21 ppbv, respectively. Generally, high concentrations of CO and SO_2 were observed in winter and spring. The measured NO and NO_2 concentrations varied from 0.4 to 51 ppbv and 1 to 79 ppbv, respectively. In general, the high NO and NO_2 concentrations were observed in autumn and winter. The TVOCs concentrations estimated with all the measured VOCs varied between 9 and 393 ppbv during the observation period and the high values were measured in autumn and winter. More details about the abovementioned parameters will be discussed in the following section.

3.2 Concentration and composition of VOCs

In total 100 VOCs were observed in Nanjing industrial area, including 27 alkanes, 11 alkenes, 1 alkyne, 17 aromatics, 31 halocarbons, 12 OVOCs, and 1 other (carbon disulfide) (Table S2). Ethane (5.8±2.5 ppbv), propane (4.2±1.5 ppbv), and ethylene (3±1.6 ppbv) were the most abundant VOCs in the study area during the observation period. However, we observed season-wise variations in the order of abundant VOC species (Table S2). For instance, acetone was the 3rd highest concentrated VOC in spring. The abovementioned 4 VOC species are also frequently mentioned as the most abundant VOCs in different regions in China (Deng et al., 2019; He et al., 2019; J. Li et al., 2018; Ma et al., 2019). We compared the individual VOC concentrations with the available data presented in recent investigations. The individual VOC concentrations in the current observation were similar to those in the previous investigations in the same study area, however, they were almost twice of those found in a nonindustrial suburban area in Nanjing (Table S2). Some of the differences in comparison to the study performed in nonindustrial suburban area in Nanjing (Wu et al., 2020) may be due to the differences in observation period. The yearly concentrations reported in the study performed in nonindustrial suburban area in Nanjing were probably estimated over a continuous measurement data for a year. However, the yearly concentrations in the current observation were estimated using the data which were not continusly measured during all the days of a year. The autumn time individual VOC concentrations in the current observation were about 1.4 fold lower than those measured in Beijing during October-November (Li et al., 2015). The winter time individual VOC concentrations in the current observation were also about 1.4 fold lower than those measured in ~~and~~ Shanghai during November-January (Zhang et al., 2018). ~~, but~~But, the yearly individual VOC concentrations in the current observation were similar to those measured in Guangzhou during June-May (Zou et al., 2015). During the observation period, the concentrations of different VOC-groups were in the order of alkanes (21±7 ppbv, 35%)> halocarbons (14.3±7.3 ppbv, 24%)> aromatics (9.9±5.8 ppbv, 17%)> OVOCs (7.5±1.9 ppbv, 13%)> alkenes (5±1.9 ppbv, 8%)> alkynes (1.4±0.3 ppbv, 2%)> others (0.5±0.2 ppbv, 1%). However, we noticed relatively higher proportions of OVOCs (14% and 18%) than the aromatics (12% and 14%) in summer and spring (Fig. 2c & f). The relatively higher contribution of OVOCs in summer and spring could be related to the biogenic emissions (e.g. acetone, MEK from trees). Indeed, the relative contribution of acetone and MEK to the TVOCs were higher in summer and spring than those in

autumn and winter (Table S2). Huang et al. (2019) reported that the industries, biogenic emissions, and secondary formation are the main source of OVOCs in southern China. Relatively high proportions of h~~e~~alo~~hydro~~carbons and aromatics were observed in autumn (25.7 and 19.3%, respectively) and winter (25.8 and 17.6%, respectively) compared to those measured in summer (20.4 and 11.8%, respectively) and spring (20.3 and 13.6%, respectively) (Fig. 2f). The high proportions of h~~ae~~lo~~hydro~~carbons and aromatics in autumn and winter could be related to the burning of biomass and fossil fuel for additional heating. Similar to the observation in the current study, the alkane is generally the most abundant VOC group in China (Mozaffar & Zhang, 2020). The relatively high contribution from halocarbons to the TVOCs could be related to the industrial emissions in the study area. In previous studies in an iron smelt plant in Liaoning, China, a high concentration of halocarbons (49%) was observed (Shi et al., 2015). However, halocarbons and OVOCs were not measured in previous investigations in the same study area (An et al., 2014; An et al., 2017; Shao et al., 2016) and also in another suburban area in Nanjing (Wu et al., 2020). Either aromatics or alkenes was mentioned as the second most abundant VOC-group in those studies in Nanjing, which is the 3rd and 5th most abundant VOC group in the current investigation. In Shanghai, a nearby city, alkanes (42%) and alkenes (26%) were two major VOC-groups and halocarbons and OVOCs were not reported (Zhang et al., 2018). The TVOCs concentration including halocarbons was 59.8±28.6 ppbv over the whole observation period, and relatively higher TVOCs concentrations were measured in autumn (83±20 ppbv) and winter (77.5±16.8 ppbv) compared to those in spring (39.6±13.1 ppbv) and summer (38.8±10.2 ppbv). The TVOCs concentration without halocarbons were 45.4±20.4, 61.7±14.6, 57.4±11.8, 31.6±10.9, and 30.9±8.2 ppbv during the whole observation period, autumn, winter, spring and summer, respectively. ~~About 1.5-times higher TVOCs concentration was observed relative to the previous investigation in the same study area (An et al., 2014; An et al., 2017). Besides, we also found 3-times higher TVOCs concentration compared to the one in a nonindustrial suburban area in Nanjing (Wu et al., 2020).~~ As mentioned before, ~~H~~halocarbons and OVOCs were not ~~measured~~ reported in the previous investigation in the same study area (An et al., 2014; An et al., 2017) and in a nonindustrial suburban area in Nanjing (Wu et al., 2020). The current TVOCs concentration without halocarbons and OVOCs was similar to the previous investigation in the same study area, however, 2 folds higher than the one reported in the nonindustrial suburban area in Nanjing ~~those previous studies in Nanjing, it could be one of the reasons for the relatively high~~

~~TVOCs concentration in the current study~~. Observed autumn time ~~and wintertime~~ TVOCs concentrations including halocarbons ~~were~~ was similar to ~~those~~ the one measured in urban Beijing (86.2 ppbv ~~in autumn~~during 17-31 October) (Li et al., 2015). ~~and~~ Winter time TVOCs concentrations without OVOCs in Shanghai (94.1 ppbv during~~in winter~~Nov-Jan) was higher than the current observation (70±15.1 ppbv) ~~(Li et al., 2015; (~~Zhang et al., 2018). ~~Similarly, o~~Observed summertime TVOCs concentration was similar to those found in urban Xi'an (42.6 ppbv, estimation includes halocarbons and OVOCs), Wuhan (43.9 ppbv estimation includes halocarbons and OVOCs) (Zeng et al., 2018; Sun et al., 2019). Yearly TVOCs concentration including halocarbons and OVOCs was 1.7 folds higher than the one found in Wuhan (Hui et al., 2018b). Besides, yearly TVOCs concentration (37.9 ppbv) without halocarbons and OVOCs was similar to Lanzhou, Chengdu, and Tokyo, however, 1.5 times higher than those reported for Tianjin and Ningbo (Jia et al., 2016;~~(~~Hui et al., 2018b;~~)~~ B. Liu et al., 2016a; Hoshi et al., 2008; Mo et al., 2017; Song et al., 2018). ~~However, yearly TVOCs concentration was 1.5-3 folds higher than those in Lanzhou, Wuhan, Tianjin, Ningbo, Chengdu, London, Los Angeles, and Tokyo (Jia et al., 2016; Hui et al., 2018; B. Liu et al., 2016a; Mo et al., 2017; Song et al., 2018; von Schneidemesser et al., 2010; Warneke et al., 2012; Hoshi et al., 2008).~~ The diurnal variation of the TVOCs, alkenes, aromatics, halocarbons, OVOCs, and alkanes concentrations showed a double-hump structure (Fig. 2a, b, d, & e). This double-hump pattern indicates the contribution of traffic emission during the rush-hours in the morning and evening. The lowest concentration of the TVOCs and different VOC-groups reached 12:00-16:00. Oppositely, the highest concentration of O_3 reached at that period (Fig. 3). The lowest O_3 concentrations were observed in winter which was consistent with the solar radiations.

3.3 Sources of VOCs

~~3.3.1 Specific Ratios~~

~~The use of the toluene/benzene (T/B) ratio is one of the simplest ways to preliminary analyse the VOC sources. If the T/B ratio is < 2, the study area is mainly affected by vehicle emissions (Hui et al., 2018, 2019). If the T/B ratio is > 2, the study area is influenced by other sources (e.g. industry, solvent utilization) beside vehicle emissions (Kumar et al., 2018; Niu et al., 2012; Li et al., 2019). Moreover, the T/B ratios are ranged between 0.2-0.6 in coal and biomass burning affected areas (Wang et al., 2009; Akagi et al., 2011). The diurnal variations in T/B ratios during~~

~~different seasons are depicted in Fig. 4 (a, b, c, & d). The mean values of T/B ratios were ranged between 0.9-2 (1.4±0.3), 1.3-2 (1.7±0.2), 1.1-1.6 (1.4±0.1), and 1.4-2.7 (1.9±0.3) during summer, autumn, winter, and spring, respectively. As the mean values of T/B ratios were around 2, the study area could be mainly affected by vehicle emissions. The double-hump pattern in the diurnal variations in T/B ratios also indicates that the rush-hour traffic had a significant influence on the VOCs concentrations in the study area. Besides, the 75th percentiles of T/B ratios were above 2 most of the investigation periods, therefore, the study area could also be influenced by industrial emissions.~~

~~Figure 4 (e, f, g, & h) shows the ratios of different alkanes and aromatics to acetylene. Acetylene is a tracer of combustion sources, the ratios of different alkanes and aromatics to acetylene are used to comprehend the contribution of other sources to combustion sources. The mean ratios of propane, n-butane, and i-butane to acetylene were around 2.0-4.0, 0.7-1.6, and 0.4-0.8, respectively during all the seasons, which were smaller than those (11.5, 1.8, and 2.6, respectively) observed in Guangzhou city centre, which was affected by liquefied petroleum gas (LPG) emissions (Zhang et al., 2013). Therefore, LPG usages probably contributed a little fraction to the alkanes in the study area. The mean ratios of benzene, toluene, C8-aromatics, and C9-aromatics to acetylene were around 0.3-1.0, 0.4-1.1, 0.2-0.6, and 0.1, respectively during all the seasons. The observed ratios of benzene and toluene to acetylene were much higher than those found in Jianfeng Mountains in Hainan (0.2 and 0.1, respectively) but comparable to those measured in urban Guangzhou (0.4 and 0.4-1, respectively) (Tang et al., 2007). Besides, the observed ratios of C8-aromatics and C9-aromatics to acetylene were comparable to traffic emission influenced urban Guangzhou (0.68 and 0.2, respectively) and Wuhan (0.5 and 0.2, respectively) (Zhang et al., 2013; Hui et al., 2018). Therefore, vehicle exhaust probably contributed significantly to the aromatics in the study area.~~

3.3.2 Potential Source Contribution Function (PSCF)

Besides the local sources, both the long and short distance transport of air mass could bring VOCs to the study area. Figure 5 shows the wind cluster and PSCF analysis results for different seasons. During summer, the major air mass~~es were~~ was short-distance transports from the south~~west~~ (~~40~~44%) direction and two long distance transports from southeast (~~39~~31 and 25%) directions. ~~A minor air mass (21%) was transported from the east direction.~~ High PSCF values

were in the nearby south~~west, and~~ southeast, ~~and east~~ directions; therefore, VOC pollution in the study area was mainly affected by the short-distance transport from the south and east directions. During autumn, the dominant air masses were short-distance transport from the ~~northeast~~ northwest (~~59~~35%) and long distance transport from the north~~west~~ (~~30~~34%) directions. However, according to the PSCF analysis, VOC pollution was mainly influenced by the short distance transport from the south ~~and east~~ direction~~s~~. During winter, short-distance transport~~s~~ from the ~~northeast (46%) and~~ northwest (~~37~~52%) direction~~s~~ ~~were~~ was the major incoming air masses to the study area. According to the PSCF values, the short-distance air masses from the south and ~~east~~ north directions were mainly transported VOC to the receptor site. During spring, air mass was mainly transported from the ~~southwestern~~ north (~~49~~50%) and ~~eastern~~ southwest (~~30~~32%) directions. A minor long distance air mass transported from the northwest (18%) direction. Atmospheric VOCs to the study area were mainly transported by these ~~two~~ air masses mostly from the nearby areas. Overall, the high PSCF values were concentrated around the measurement site, therefore, short distance transports from the surrounding areas and cities were the main reason for the high VOC concentration. The above conclusion perfectly makes sense as the sampling site is surrounded by different chemical and petrochemical industries, steel plants, gas stations, high traffic roads, and residential areas.

3.3.3 PMF Model Analysis

~~Differences were observed among the source profiles of VOCs obtained for different seasons (Sect. S1). For instance, the biogenic source was identified in summer, biomass burning source was distinguished in autumn, and LPG/NG usage source was found in winter and spring. However, industry and vehicle-related VOC sources were identified during all the measurement seasons. According to PMF model results, aromatics were emitted from solvent usages, vehicle, and industry-related sources. Besides, industry and combustion processes were the main sources of halocarbons and OVOCs. Moreover, alkanes and alkenes were emitted from vehicle exhaust and fuel usage sources.~~

~~Figure 6 shows the relative contributions of different sources to ambient VOCs during different seasons. Overall, industry related sources contributed to the major portion of the ambient VOC concentrations followed by vehicle emission. Industrial emission accounted for about 32%, 47%,~~

~~45%, and 23% in summer, autumn, winter, and spring, respectively. The contributions of vehicle emission were about 34%, 26%, 24%, and 27% in summer, autumn, winter, and spring, respectively. The contribution of vehicle emission remained similar during the 4 seasons, however, the contribution of the industrial emission increased in autumn and winter. Previous investigations performed in Beijing, Tianjin, Wuhan, Chengdu, and Shuozhou also found that the industry and vehicle are the two most important VOC sources (Zhang et al. 2017; Liu et al. 2016; Hui et al. 2018; Song et al. 2018) Jia et al., 2016). Besides these two sources, solvent usage (11%, 10%, 10%, and 4%, respectively) and gasoline evaporation (17%, 10%, NA, 6%, respectively) were two important VOC sources during those 4 seasons. Moreover, source contribution from the biogenic source in summer (7%), biomass burning in autumn (7%), LPG/NG usage in winter (11%) and spring (18%), and multiple sources in winter (10%) and spring (23%) was observed.~~

According to the PMF model analysis, five VOC sources were common during all the measurement seasons. They were biomass/biofuel burning, LPG/NG usage, gasoline evaporation, gasoline vehicle exhaust, and paint solvent usage (Sect. S1). The biogenic source was identified in summer. Figure 6 shows the relative contributions of different sources to ambient VOCs during different seasons. Overall, vehicle-related sources contributed to the major portion of the ambient VOC concentrations. The total contributions of vehicle-related emission were about 39%, 33%, 48%, and 42% in summer, autumn, winter, and spring, respectively. The contributions of biomass/biofuel burning were about 19%, 21%, 17%, and 16.4% in summer, autumn, winter, and spring, respectively. Besides these two sources, LPG/NG usage (18%, 21%, 16%, and 18%, respectively) and paint solvent usage (8%, 12%, 11%, 5%, respectively) were two important VOC sources during those 4 seasons.

3.4 Chemical reactivity (L_{OH}) ~~and contribution to O_3 and SOA formation~~

The estimated loss rates of OH radical (L_{OH}) with VOCs were about 2-fold high in autumn (13.7 s^{-1}) and winter (13.5 s^{-1}) compared to those in summer (7 s^{-1}) and spring (7.5 s^{-1}) (Fig. 7 a). The relatively high L_{OH} values in autumn and winter were due to the relatively high VOC concentrations in those seasons (Fig.2). The average L_{OH} value was 10.4±3.6 s^{-1} over the four seasons. It was in a similar range with the values determined in Guangzhou (10.9 s^{-1}), Chongqing (10 s^{-1}), Xian (1.6-16.2 s^{-1}), and Tokyo (7.7-13.4 s^{-1}), however, higher than the values estimated

in Shanghai (2.9-5 s^{-1}, 6.2 s^{-1}) and Beijing (7 s^{-1}) (Tan et al., 2019; Zhu et al., 2019; Yoshino et al., 2012; Song et al., 2020). While alkene was the highest contributor to the L^{OH} in summer (3 s^{-1}, 43%) and spring (2.6 s^{-1}, 35%), aromatic was the maximum contributor in autumn (6.9 s^{-1}, 50%) and winter (5.9 s^{-1}, 44%) (Fig. 11 a & d). An increase in the OH loss rate by OVOCs was observed in spring (17%) compared to the other seasons (10, 8, and 9% in summer, autumn, and winter, respectively). Over the four seasons, the contribution of VOC-groups to L_{OH} exhibited the following trend: aromatics > alkenes > alkanes > OVOCs > halocarbons. Similar to the current study, aromatic is also mentioned as the maximum contributors to L_{OH} in different regions in China, however, the alkene is generally reported as the top contributor to L_{OH} (Zhang et al., 2020; Zhao et al., 2020; Hui et al., 2018; Song et al., 2020). Figure 7 also shows the top 10 VOCs contributing to L_{OH} for different seasons. Whereas isoprene was the highest contributor to L_{OH} in summer, styrene was the largest contributor in autumn and winter. On the other hand, naphthalene was the main contributor to L^{OH} in spring. Overall, styrene, naphthalene, ethylene, and isoprene were the main contributor to L_{OH} in the study area. In previous studies in China, these compounds are also mentioned as one of the highest contributors to L_{OH} (Zhao et al., 2020; Hui et al., 2018; Song et al., 2020).

~~The estimated O_3 formation potential (OFP) of VOCs were about 2 times high in autumn (170.8 ppbv) and winter (175.4 ppbv) relative to those in summer (86.2 ppbv) and spring (82.8 ppbv) (Fig. 8 a). The average OFP value was 128.8±51.2 ppbv during the measurement period. The springtime OFP was similar to the one estimated in Beijing (80 ppbv) (Li et al., 2015). The summertime OFP was about 1.5 times higher than the one in Xi'an (Song et al., 2020), but, about 1.4-2 folds lower than those found in Shanghai (Liu et al., 2019). The average OFP was about 1.5 times higher than the one in Wuhan (Hui et al., 2018). Whereas alkene was the major contributor to OFP in summer (37.4 ppbv, 43%), winter (72.8 ppbv, 41%), and spring (31.6 ppbv, 38%), aromatics contributed the most to OFP in autumn (62.7 ppbv, 37%) (Fig. 12 a & d). During the measurement period, the contribution of VOC-groups to OFP showed the following trend: alkenes > aromatics > alkanes > OVOCs > halocarbons. The alkene is also mentioned as the top contributor to OFP in Nanjing and the same observation is commonly found in China (An et al., 2014; Hui et al., 2018; Song et al., 2018; Song et al., 2020). The top 10 VOCs contributing to OFP for different seasons are also shown in Fig. 8 (b, c, e, & f). Ethylene was the major contributor to OFP during all the season. Followed by ethylene, cis-1,3-dichloropropene was the~~

~~main contributor to OFP from summer to winter. In spring, propylene was the second most contributors to OFP. Overall, different alkenes were the highest contributor to OFP in the study area. Alkenes are also mentioned as the top contributor to OFP in the previous investigations in Nanjing (An et al., 2014). Therefore, the reduction of these alkenes emissions in the study area could be one of the ways to reduce ambient O_3 concentration.~~

~~The secondary organic aerosol potentials (SOAP) were about 3 times higher in autumn (1422 ppbv) and winter (1269 ppbv) than those in summer (466 ppbv) and spring (398 ppbv) (Fig. 9a). The average SOAP was 889±531 ppbv during the measurement period. The average SOAP was about 2-3 times higher than those estimated in Wuhan and Beijing (Hui et al., 2019; Li et al., 2020). Aromatics was the main contributor to SOAP during all the seasons (95-97%) (Fig. 9 a & d) which was consistent with the observations in Chengdu (Song et al., 2018), Beijing (Li et al., 2020), and Wuhan (Hui et al., 2019). During the measurement period, the contribution of VOC groups to SOAP exhibited the following trend: aromatics > alkanes > alkenes > OVOCs. Styrene, cumene, toluene, benzene, and o-xylene were the major contributor to SOAP during all the season (Fig. 9 b, c, e, & f). Therefore, the reduction of these aromatics emissions in the study area could be one of the ways to reduce ambient SOA concentration.~~

3.5 Sensitivity analysis of O_3 formation

Figure 10 shows the EKMA isopleth diagrams of O_3 for different seasons. In all the diagrams, VOC and NOx = 100 % is the base case. The ridgeline divided the diagrams into two regimes, VOC-sensitive (above) and NOx-sensitive (below) regimes. For all the seasons, the study area fell above the ridgeline. Moreover, a decrease in O_3 production was noticed with the decrease in VOC concentration. Therefore, the study area was in the VOC-sensitive regime for O_3 formation during all the seasons. As a case study, O_3 formation sensitivity to its precursors was tested on a high O_3 concentration day (July 29 2018, maximum 126 ppbv). During the high O_3 episode, the study area was also in the VOC-sensitive regime for O_3 formation (Fig. S5). We also employed the RIR analysis to evaluate the O_3 production sensitivity to VOC, NOx, and CO concentrations (Fig. 11). The RIR value of VOC was the highest during all the seasons. It indicates that the O_3 production was more sensitive to the reduction of VOC concentration. This finding is consistent with the above results in the EKMA isopleth (Fig. 10). Except for the spring, the RIR values of CO were very small relative to those for the VOC. It indicates that the CO concentrations were

relatively less important for the O_3 formation during those seasons. The RIR values for NOx were negative during all the seasons, implying that the O_3 formation was in the NOx-titration regime in the study area. From the above analysis, it is evident that a reduction of VOC concentration in the study area will be the most efficient way to reduce the O_3 formation. The previous two studies performed in Nanjing also concluded the same finding based on VOC/NOx ratios and RIR analysis (An et al., 2015; Xu et al., 2017). Our findings are also consistent with the previous studies performed in other regions in China (Tan et al., 2018a; He et al., 2019; Feng et al., 2019; Ma et al., 2019). However, NOx-sensitive regions for O_3 formation are also found in China (Tan et al., 2018; Jia et al., 2016).

4 Conclusions

Industries are an important anthropogenic source of VOCs. VOC plays a major role in tropospheric chemistry and air quality. Nanjing is one of the biggest industrial cities in China. We performed a long term investigation of ambient VOCs in an industrial area in Nanjing. ~~About 1.5~~Similar and ~~3~~2-folds high TVOCs concentrations were observed compared to those previously reported in the same study area and a nonindustrial suburban area in Nanjing, respectively. ~~The relatively high TVOCs was due to halocarbons and OVOCs concentrations were not measured in those previous studies in Nanjing. Therefore, halocarbons and OVOCs were an important part of the TVOCs in Nanjing, and industrial emissions had a large influence on VOC concentration in the study area.~~ Observed TVOCs concentration was also ~~about 1.5~~similar ~~3~~ 1.7 folds higher than those reported in other cities in China and the world, but, ~~similar~~ 1.3 times smaller ~~to~~ than ~~those~~ the one measured in urban ~~Beijing and~~ Shanghai. This high VOC concentration in the study area needs to be reduced to decrease O_3 concentration and improve the local air quality. TVOCs concentrations were about 2-times high in autumn and winter compared to those in summer and spring. Generally, haze pollutions frequently happen in autumn and winter, therefore, VOC concentration reduction in these seasons is an important step to reduce haze pollutions in the study area. After alkane, halocarbon was the 2nd largest contributor to the TVOCs, indicating a high influence of industrial emissions. Generally, alkenes/aromatics/OVOCs are the 2nd largest contributor to the TVOCs in China, therefore, industries in Nanjing emitted a high amount of halocarbons into the atmosphere. As halocarbons are carcinogenic, their emissions should be reduced. PSCF analysis indicated that the short

distance transports from the surrounding areas and cities were the main reason for high VOC concentration in the study area. Hence, local emissions should be reduced to decrease the haze and O_3 pollution in the study area. ~~Industries~~ Vehicle-related emissions were the major VOC sources in the study area ~~followed by vehicles~~, thus, emission reduction from these ~~two~~ sources should get more priority. Aromatics and alkenes accounted for most of the L_{OH}, ~~OFP, and SOAP,~~ thus, these 2 kinds of VOCs should get more priority in emission reduction policies and strategies. During all the seasons, the study area was in the VOC-sensitive regime for O_3 formation. Therefore, VOCs especially aromatics and alkenes emission reduction is the most effective way to decrease the local O_3 formation.

Data availability

All the data presented in this article can be accessed through https://osf.io/bm6cs/.

Author contribution

YLZ designed and supervised the project; MYF, FX, YCL, FC, and AM conducted the measurements; AM analysed the data and prepared the manuscript. All authors contributed in discussion to improve the article.

Competing interests

The authors declare that they have no conflict of interest.

Acknowledgements

The authors thank funding support from the National Nature Science Foundation of China (No. 41977305 and 41761144056), the Provincial Natural Science Foundation of Jiangsu (No. BK20180040), and the Jiangsu Innovation & Entrepreneurship Team. We are also grateful to Zijin Zhang and Meng-Yao Cao for their help on sampling.

References

An, J., Wang, J., Zhang, Y., & Zhu, B. (2017). Source Apportionment of Volatile Organic Compounds in an Urban Environment at the Yangtze River Delta, China. *Archives of Environmental Contamination and Toxicology*, *72*(3), 335–348.

https://doi.org/10.1007/s00244-017-0371-3

An, J., Zhu, B., Wang, H., Li, Y., Lin, X., & Yang, H. (2014a). Characteristics and source apportionment of VOCs measured in an industrial area of Nanjing, Yangtze River Delta, China. *Atmospheric Environment*, *97*, 206–214. https://doi.org/10.1016/j.atmosenv.2014.08.021

An, J., Zhu, B., Wang, H., Li, Y., Lin, X., & Yang, H. (2014b). Characteristics and source apportionment of VOCs measured in an industrial area of Nanjing, Yangtze River Delta, China. *Atmospheric Environment*, *97*, 206–214. https://doi.org/https://doi.org/10.1016/j.atmosenv.2014.08.021

An, J., Zou, J., Wang, J., Lin, X., & Zhu, B. (2015). Differences in ozone photochemical characteristics between the megacity Nanjing and its suburban surroundings, Yangtze River Delta, China. *Environmental Science and Pollution Research*, *22*(24), 19607–19617. https://doi.org/10.1007/s11356-015-5177-0

Cardelino, C. A., & Chameides, W. L. (1995). An observation-based model for analyzing ozone precursor relationships in the urban atmosphere. *Journal of the Air and Waste Management Association*, *45*(3), 161–180. https://doi.org/10.1080/10473289.1995.10467356

Carter, W. P. L. (2010). Development of the SAPRC-07 chemical mechanism. *Atmospheric Environment*, *44*(40), 5324–5335. https://doi.org/10.1016/j.atmosenv.2010.01.026

Chen, Y., Ge, X., Chen, H., Xie, X., Chen, Y., Wang, J., … Chen, M. (2018). Seasonal light absorption properties of water-soluble brown carbon in atmospheric fine particles in Nanjing, China. *Atmospheric Environment*, *187*(June), 230–240. https://doi.org/10.1016/j.atmosenv.2018.06.002

Deng, Y., Li, J., Li, Y., Wu, R., & Xie, S. (2019). Characteristics of volatile organic compounds, NO2, and effects on ozone formation at a site with high ozone level in Chengdu. *Journal of Environmental Sciences (China)*, *75*(2), 334–345. https://doi.org/10.1016/j.jes.2018.05.004

Feng, R., Wang, Q., Huang, C. chen, Liang, J., Luo, K., Fan, J. ren, & Zheng, H. jun. (2019). Ethylene, xylene, toluene and hexane are major contributors of atmospheric ozone in Hangzhou, China, prior to the 2022 Asian Games. *Environmental Chemistry Letters*, *17*(2), 1151–1160. https://doi.org/10.1007/s10311-018-00846-w

Feng, T., Bei, N., Huang, R. J., Cao, J., Zhang, Q., Zhou, W., … Li, G. (2016). Summertime ozone formation in Xi'an and surrounding areas, China. *Atmospheric Chemistry and*

Physics, *16*(7), 4323–4342. https://doi.org/10.5194/acp-16-4323-2016

He, Z., Wang, X., Ling, Z., Zhao, J., Guo, H., Shao, M., & Wang, Z. (2019). Contributions of different anthropogenic volatile organic compound sources to ozone formation at a receptor site in the Pearl River Delta region and its policy implications. *Atmospheric Chemistry and Physics*, *19*(13), 8801–8816. https://doi.org/10.5194/acp-19-8801-2019

Huang, X., Wang, C., Zhu, B., Lin, L., & He, L. (2019). Exploration of sources of OVOCs in various atmospheres in southern. *Environmental Pollution*, *249*, 831–842. https://doi.org/10.1016/j.envpol.2019.03.106

Hui, L., Liu, X., Tan, Q., Feng, M., An, J., Qu, Y., … Cheng, N. (2019). VOC characteristics, sources and contributions to SOA formation during haze events in Wuhan, Central China. *Science of the Total Environment*, *650*, 2624–2639. https://doi.org/10.1016/j.scitotenv.2018.10.029

Hui, L., Liu, X., Tan, Q., Feng, M., An, J., Qu, Y., … Jiang, M. (2018a). Characteristics, source apportionment and contribution of VOCs to ozone formation in Wuhan, Central China. *Atmospheric Environment*, *192*(August), 55–71. https://doi.org/10.1016/j.atmosenv.2018.08.042

Hui, L., Liu, X., Tan, Q., Feng, M., An, J., Qu, Y., … Jiang, M. (2018b). Characteristics, source apportionment and contribution of VOCs to ozone formation in Wuhan, Central China. *Atmospheric Environment*, *192*(2), 55–71. https://doi.org/10.1016/j.atmosenv.2018.08.042

Hung-Lung, C., Jiun-Horng, T., Shih-Yu, C., Kuo-Hsiung, L., & Sen-Yi, M. (2007). VOC concentration profiles in an ozone non-attainment area: A case study in an urban and industrial complex metroplex in southern Taiwan. *Atmospheric Environment*, *41*(9), 1848–1860. https://doi.org/https://doi.org/10.1016/j.atmosenv.2006.10.055

Jenkin, M. E., Young, J. C., & Rickard, A. R. (2015). The MCM v3.3.1 degradation scheme for isoprene. *Atmospheric Chemistry and Physics*, *15*(20), 11433–11459. https://doi.org/10.5194/acp-15-11433-2015

Jenkin, Michael E., Saunders, S. M., & Pilling, M. J. (1997). The tropospheric degradation of volatile organic compounds: A protocol for mechanism development. *Atmospheric Environment*, *31*(1), 81–104. https://doi.org/10.1016/S1352-2310(96)00105-7

Jia, C., Mao, X., Huang, T., Liang, X., Wang, Y., Shen, Y., … Gao, H. (2016). Non-methane hydrocarbons (NMHCs) and their contribution to ozone formation potential in a

petrochemical industrialized city, Northwest China. *Atmospheric Research*, *169*, 225–236. https://doi.org/10.1016/j.atmosres.2015.10.006

Li, J., Xie, S. D., Zeng, L. M., Li, L. Y., Li, Y. Q., & Wu, R. R. (2015). Characterization of ambient volatile organic compounds and their sources in Beijing, before, during, and after Asia-Pacific Economic Cooperation China 2014. *Atmospheric Chemistry and Physics*, *15*(14), 7945–7959. https://doi.org/10.5194/acp-15-7945-2015

Li, Jing, Zhai, C., Yu, J., Liu, R., Li, Y., Zeng, L., & Xie, S. (2018). Spatiotemporal variations of ambient volatile organic compounds and their sources in Chongqing, a mountainous megacity in China. *Science of the Total Environment*, *627*, 1442–1452. https://doi.org/10.1016/j.scitotenv.2018.02.010

Liu, B., Liang, D., Yang, J., Dai, Q., Bi, X., Feng, Y., … Xu, H. (2016). Characterization and source apportionment of volatile organic compounds based on 1-year of observational data in Tianjin, China. *Environmental Pollution*, *218*, 757–769. https://doi.org/10.1016/j.envpol.2016.07.072

Ma, Z., Liu, C., Zhang, C., Liu, P., Ye, C., Xue, C., … Mu, Y. (2019). The levels , sources and reactivity of volatile organic compounds in a typical urban area of Northeast China. *Journal of Environmental Sciences*, *79*, 121–134. https://doi.org/10.1016/j.jes.2018.11.015

Meng, H. A. N., Xueqiang, L. U., Chunsheng, Z., Liang, R. A. N., & Suqin, H. A. N. (2015). Characterization and Source Apportionment of Volatile Organic Compounds in Urban and Suburban Tianjin , China. *Advances in Atmospheric Sciences*, *32*(3), 439–444. https://doi.org/10.1007/s00376-014-4077-4.1.

Mo, Z., Shao, M., Lu, S., Niu, H., Zhou, M., & Sun, J. (2017). Characterization of non-methane hydrocarbons and their sources in an industrialized coastal city , Yangtze River Delta , China. *Science of the Total Environment*, *593–594*, 641–653. https://doi.org/10.1016/j.scitotenv.2017.03.123

Mozaffar, A., & Zhang, Y. L. (2020). Atmospheric Volatile Organic Compounds (VOCs) in China: a Review. *Current Pollution Reports*, *6*(3), 250–263. https://doi.org/10.1007/s40726-020-00149-1

Mozaffar, A., Zhang, Y. L., Fan, M., Cao, F., & Lin, Y. C. (2020). Characteristics of summertime ambient VOCs and their contributions to O3 and SOA formation in a suburban area of Nanjing, China. *Atmospheric Research*, *240*(February).

https://doi.org/10.1016/j.atmosres.2020.104923

Na, K., Kim, Y. P., Moon, K.-C., Moon, I., & Fung, K. (2001). Concentrations of volatile organic compounds in an industrial area of Korea. *Atmospheric Environment*, *35*(15), 2747–2756. https://doi.org/https://doi.org/10.1016/S1352-2310(00)00313-7

Petit, J. E., Favez, O., Albinet, A., & Canonaco, F. (2017). A user-friendly tool for comprehensive evaluation of the geographical origins of atmospheric pollution: Wind and trajectory analyses. *Environmental Modelling and Software*, *88*, 183–187. https://doi.org/10.1016/j.envsoft.2016.11.022

Saunders, S. M., Jenkin, M. E., Derwent, R. G., & Pilling, M. J. (2003). Protocol for the development of the Master Chemical Mechanism, MCM v3 (Part A): Tropospheric degradation of non-aromatic volatile organic compounds. *Atmospheric Chemistry and Physics*, *3*(1), 161–180. https://doi.org/10.5194/acp-3-161-2003

Shao, P., An, J., Xin, J., Wu, F., Wang, J., Ji, D., & Wang, Y. (2016). Source apportionment of VOCs and the contribution to photochemical ozone formation during summer in the typical industrial area in the Yangtze River Delta, China. *Atmospheric Research*, *176–177*, 64–74. https://doi.org/10.1016/j.atmosres.2016.02.015

Shi, J., Deng, H., Bai, Z., Kong, S., Wang, X., Hao, J., … Ning, P. (2015). Emission and profile characteristic of volatile organic compounds emitted from coke production, iron smelt, heating station and power plant in Liaoning Province, China. *Science of the Total Environment*, *515–516*(x), 101–108. https://doi.org/10.1016/j.scitotenv.2015.02.034

Song, M., Li, X., Yang, S., Yu, X., Zhou, S., Yang, Y., … Zhang, Y. (2020). Spatiotemporal Variation, Sources, and Secondary Transformation Potential of VOCs in Xi'an, China, *30*(August). Retrieved from https://doi.org/10.5194/acp-2020-704

Song, M., Tan, Q., Feng, M., Qu, Y., & Liu, X. (2018). Source Apportionment and Secondary Transformation of Atmospheric Nonmethane Hydrocarbons in Chengdu , Southwest China. *Journal of Geophysical Research Atmospheres*, *123*(2), 9741–9763. https://doi.org/10.1029/2018JD028479

Song, M., Tan, Q., Feng, M., Qu, Y., Liu, X., An, J., & Zhang, Y. (2018). Source Apportionment and Secondary Transformation of Atmospheric Nonmethane Hydrocarbons in Chengdu, Southwest China. *Journal of Geophysical Research: Atmospheres*, *123*(17), 9741–9763. https://doi.org/10.1029/2018JD028479

Sun, J., Shen, Z., Zhang, Y., Zhang, Z., Zhang, Q., Zhang, T., … Li, X. (2019). Urban VOC profiles, possible sources, and its role in ozone formation for a summer campaign over Xi'an, China. *Environmental Science and Pollution Research*, *26*(27), 27769–27782. https://doi.org/10.1007/s11356-019-05950-0

Tan, Z., Lu, K., Dong, H., Hu, M., Li, X., Liu, Y., … Zhang, Y. (2018). Explicit diagnosis of the local ozone production rate and the ozone-NOx-VOC sensitivities. *Science Bulletin*, *63*(16), 1067–1076. https://doi.org/10.1016/j.scib.2018.07.001

Tan, Z., Lu, K., Jiang, M., Su, R., Dong, H., Zeng, L., … Zhang, Y. (2018a). Exploring ozone pollution in Chengdu, southwestern China: A case study from radical chemistry to O3-VOC-NOx sensitivity. *Science of The Total Environment*, *636*, 775–786. https://doi.org/10.1016/J.SCITOTENV.2018.04.286

Tan, Z., Lu, K., Jiang, M., Su, R., Dong, H., Zeng, L., … Zhang, Y. (2018b). Exploring ozone pollution in Chengdu , southwestern China : A case study from radical chemistry to O 3 - VOC-NO x sensitivity. *Science of the Total Environment*, *636*, 775–786. https://doi.org/10.1016/j.scitotenv.2018.04.286

Tan, Z., Lu, K., Jiang, M., Su, R., Wang, H., Lou, S., … Zhang, Y. (2019). Daytime atmospheric oxidation capacity in four Chinese megacities during the photochemically polluted season: A case study based on box model simulation. *Atmospheric Chemistry and Physics*, *19*(6), 3493–3513. https://doi.org/10.5194/acp-19-3493-2019

Tiwari, V., Hanai, Y., & Masunaga, S. (2010). Ambient levels of volatile organic compounds in the vicinity of petrochemical industrial area of Yokohama, Japan. *Air Quality, Atmosphere and Health*, *3*(2), 65–75. https://doi.org/10.1007/s11869-009-0052-0

Vermeuel, M. P., Novak, G. A., Alwe, H. D., Hughes, D. D., Kaleel, R., Dickens, A. F., … Bertram, T. H. (2019). Sensitivity of Ozone Production to NOx and VOC Along the Lake Michigan Coastline. *Journal of Geophysical Research: Atmospheres*, *124*(20), 10989–11006. https://doi.org/10.1029/2019JD030842

Wolfe, G. M., Marvin, M. R., Roberts, S. J., Travis, K. R., & Liao, J. (2016). The framework for 0-D atmospheric modeling (F0AM) v3.1. *Geoscientific Model Development*, *9*(9), 3309–3319. https://doi.org/10.5194/gmd-9-3309-2016

Wu, R., Zhao, Y., Zhang, J., & Zhang, L. (2020). Variability and sources of ambient volatile organic compounds based on online measurements in a suburban region of nanjing, eastern

China. *Aerosol and Air Quality Research*, *20*(3), 606–619. https://doi.org/10.4209/aaqr.2019.10.0517

Xu, Z., Huang, X., Nie, W., Chi, X., & Xu, Z. (2017). Influence of synoptic condition and holiday effects on VOCs and ozone production in the Yangtze River Delta region , China. *Atmospheric Environment*, *168*, 112–124. https://doi.org/10.1016/j.atmosenv.2017.08.035

Yan, Y., Yang, C., Peng, L., Li, R., & Bai, H. (2016). Emission characteristics of volatile organic compounds from coal-, coal gangue-, and biomass-fired power plants in China. *Atmospheric Environment*, *143*, 261–269. https://doi.org/10.1016/j.atmosenv.2016.08.052

Yoshino, A., Nakashima, Y., Miyazaki, K., Kato, S., Suthawaree, J., Shimo, N., … Kajii, Y. (2012). Air quality diagnosis from comprehensive observations of total OH reactivity and reactive trace species in urban central Tokyo. *Atmospheric Environment*, *49*, 51–59. https://doi.org/10.1016/j.atmosenv.2011.12.029

Zeng, P., Lyu, X. P., Guo, H., Cheng, H. R., Jiang, F., Pan, W. Z., … Hu, Y. Q. (2018). Causes of ozone pollution in summer in Wuhan, Central China. *Environmental Pollution*, *241*(x), 852–861. https://doi.org/10.1016/j.envpol.2018.05.042

Zhang, F., Shang, X., Chen, H., Xie, G., Fu, Y., Wu, D., … Chen, J. (2020). Significant impact of coal combustion on VOCs emissions in winter in a North China rural site. *Science of the Total Environment*, *720*. https://doi.org/10.1016/j.scitotenv.2020.137617

Zhang, H., Li, H., Zhang, Q., Zhang, Y., Zhang, W., Wang, X., … Xia, F. (2017). Atmospheric volatile organic compounds in a typical urban area of beijing: Pollution characterization, health risk assessment and source apportionment. *Atmosphere*, *8*(3). https://doi.org/10.3390/atmos8030061

Zhang, Y., Li, R., Fu, H., Zhou, D., & Chen, J. (2018). Observation and analysis of atmospheric volatile organic compounds in a typical petrochemical area in Yangtze River. *Journal of Environmental Sciences*, *71*, 233–248. https://doi.org/10.1016/j.jes.2018.05.027

Zhang, Z., Yan, X., Gao, F., Thai, P., Wang, H., Chen, D., … Wang, B. (2018). Emission and health risk assessment of volatile organic compounds in various processes of a petroleum re fi nery in the Pearl River Delta ,. *Environmental Pollution*, *238*, 452–461. https://doi.org/10.1016/j.envpol.2018.03.054

Zhao, R., Dou, X., Zhang, N., Zhao, X., Yang, W., Han, B., … Bai, Z. (2020). The characteristics of inorganic gases and volatile organic compounds at a remote site in the

Tibetan Plateau. *Atmospheric Research*, *234*(October 2019), 104740. https://doi.org/10.1016/j.atmosres.2019.104740

Zhu, J., Wang, S., Wang, H., Jing, S., Lou, S., Saiz-Lopez, A., & Zhou, B. (2019). Observationally constrained modelling of atmospheric oxidation capacity and photochemical reactivity in Shanghai, China. *Atmospheric Chemistry and Physics Discussions*, 1–26. https://doi.org/10.5194/acp-2019-711

Zou, Y., Deng, X. J., Zhu, D., Gong, D. C., Wang, H., Li, F., … Wang, B. G. (2015). Characteristics of 1 year of observational data of VOCs, NOx and O3 at a suburban site in Guangzhou, China. *Atmospheric Chemistry and Physics*, *15*(12), 6625–6636. https://doi.org/10.5194/acp-15-6625-2015

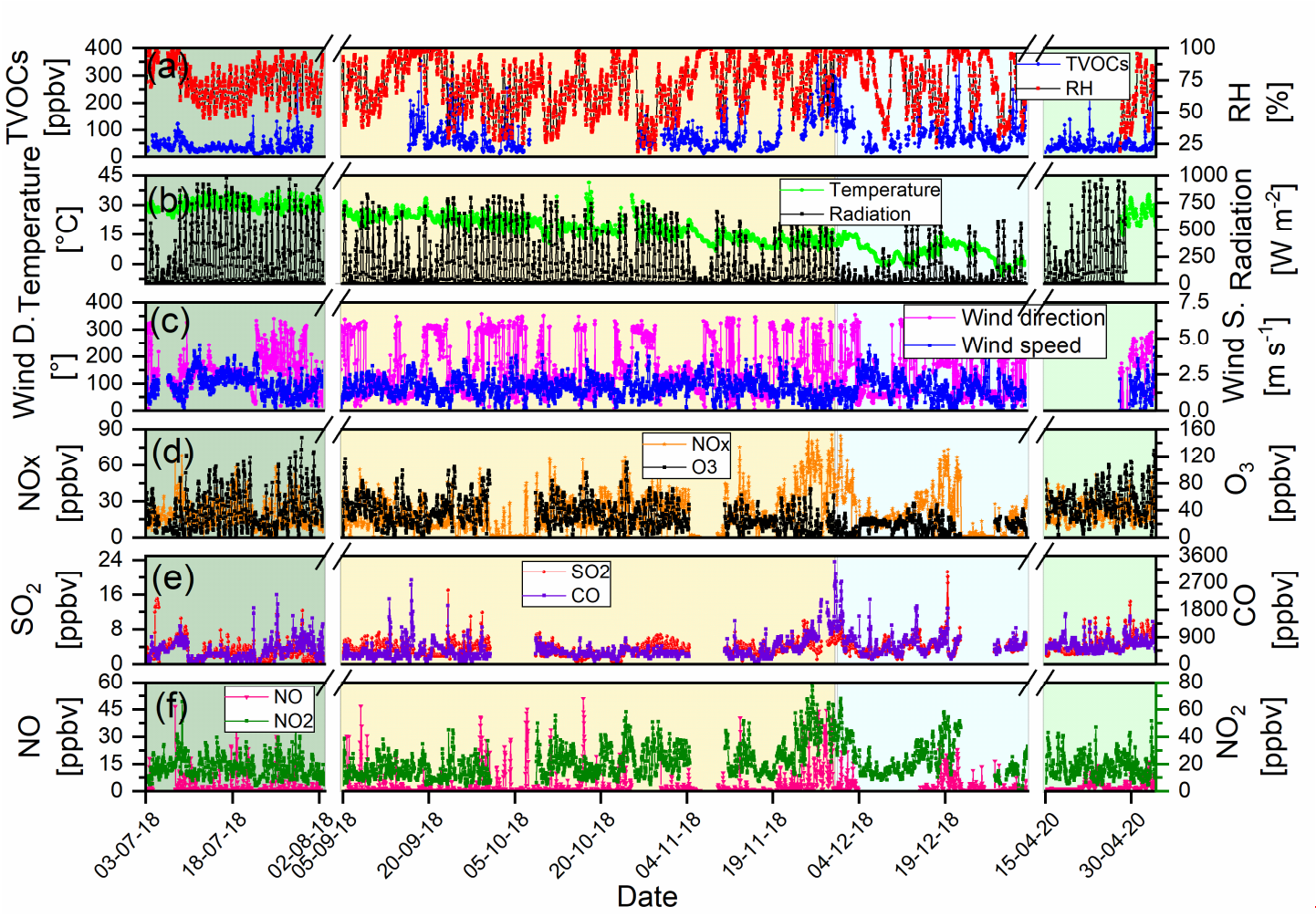
(a)
TVOCs [ppbv]
RH [%]
TVOCs
RH
(b)
Temperature [°C]
Wind S. Radiation [W m-2]
Temperature
Radiation
(c)
Wind D. [°]
Wind S. [m s-1]
Wind direction
Wind speed
(d)
NOx [ppbv]
O3 [ppbv]
NOx
O3
(e)
SO2 [ppbv]
CO [ppbv]
SO2
CO
(f)
NO [ppbv]
NO2 [ppbv]
NO
NO2
03-07-18
18-07-18
02-08-18
05-09-18
20-09-18
05-10-18
20-10-18
04-11-18
19-11-18
04-12-18
19-12-18
15-04-20
30-04-20
Date

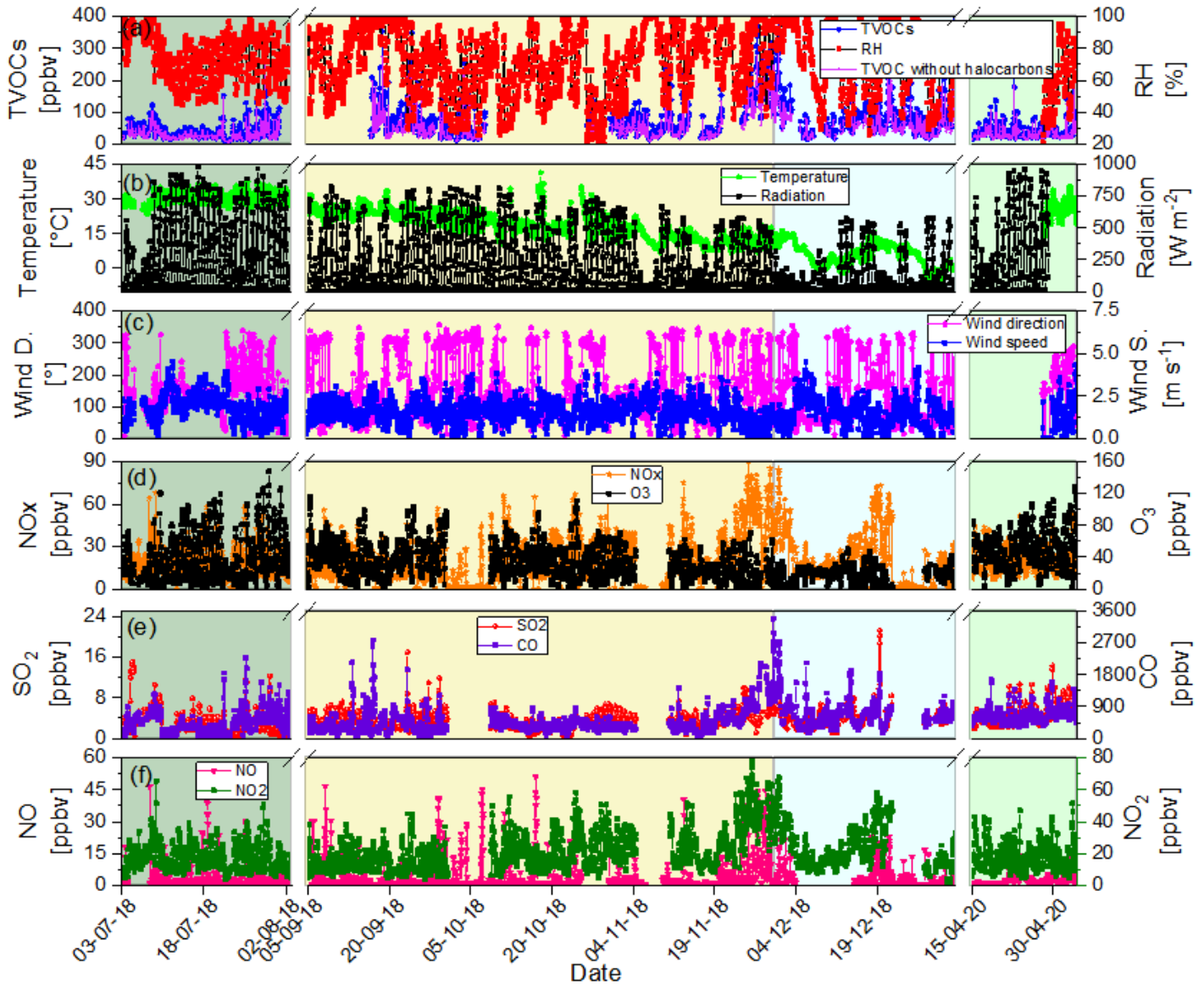

Figure 1: Time series of hourly meteorological parameters, inorganic air pollutants, ~~and~~ TVOCs, and TVOCs without halocarbons concentrations during the observation period at Nanjing. The green, yellow, cyan, and light-green shaded areas indicate summer, autumn, winter, and spring seasons, respectively. The discontinuity of the measured data is due to the instruments failure.

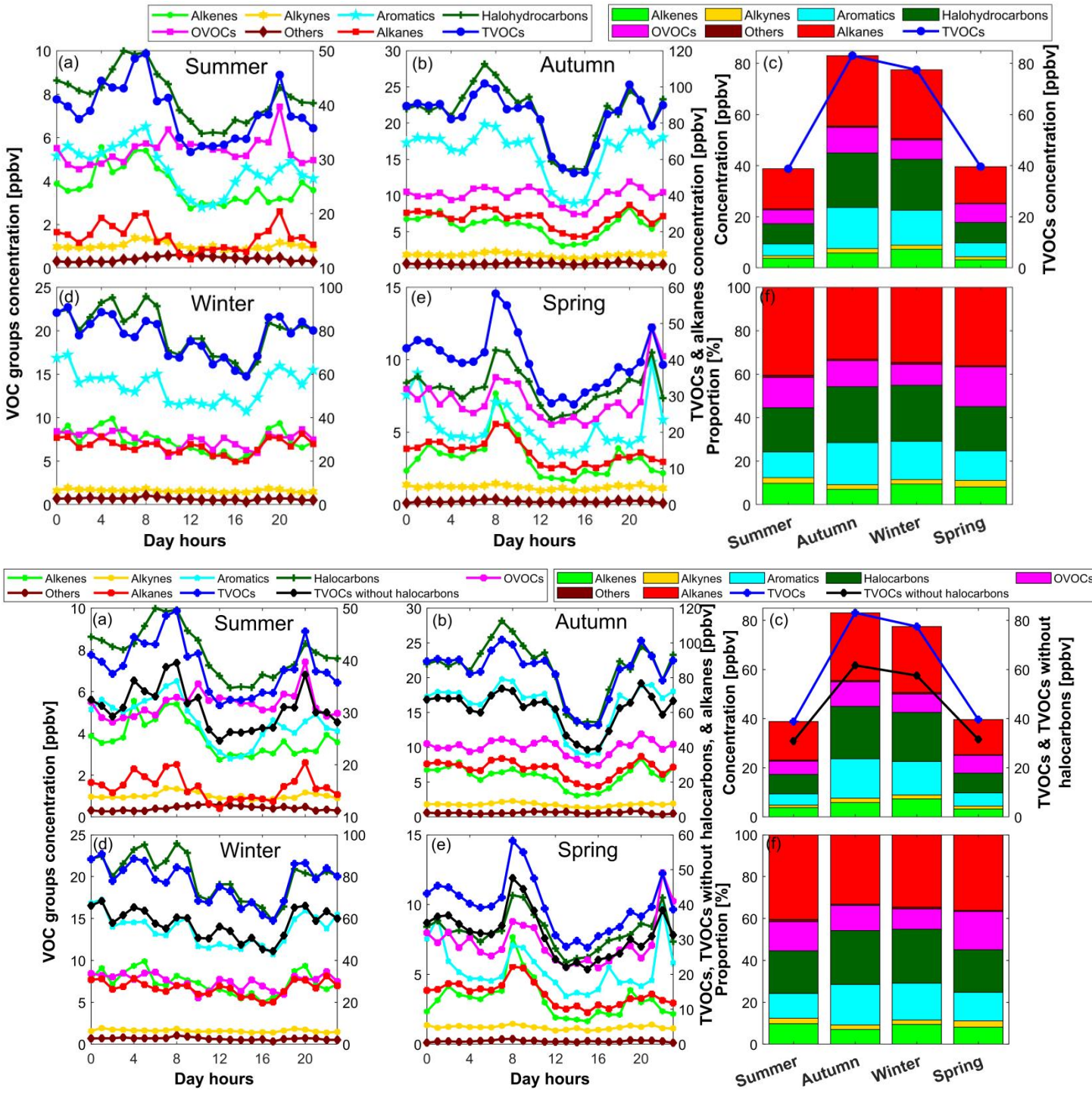

Figure 2: Diurnal variations in ~~TVOCs and~~ different VOC-groups, TVOCs, TVOCs without halocarbons concentrations in different seasons (a, b, d, & e) and seasonal variations in average concentrations and proportion of different VOC-groups, TVOCs, TVOCs without halocarbons~~TVOCs and different VOC-groups~~ (c & f).

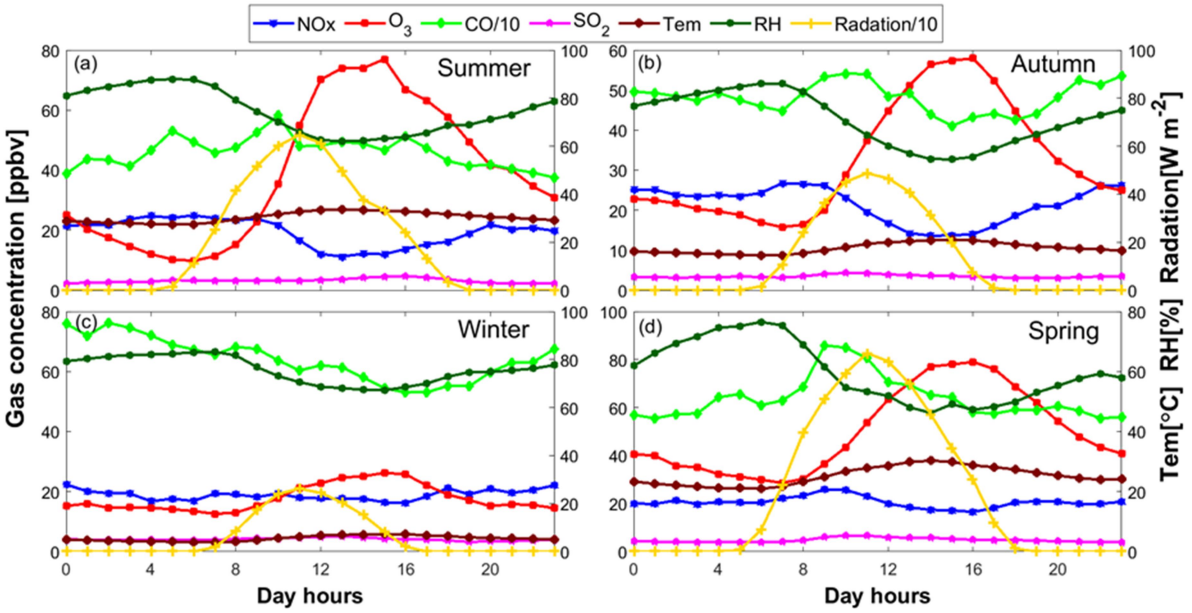

915

Figure 3: Diurnal variations in weather conditions and NOx, O3, CO, and SO2 concentrations in different seasons. Note that the plotted CO concentrations and solar radiation values are reduced by 10-folds for a better visualization.

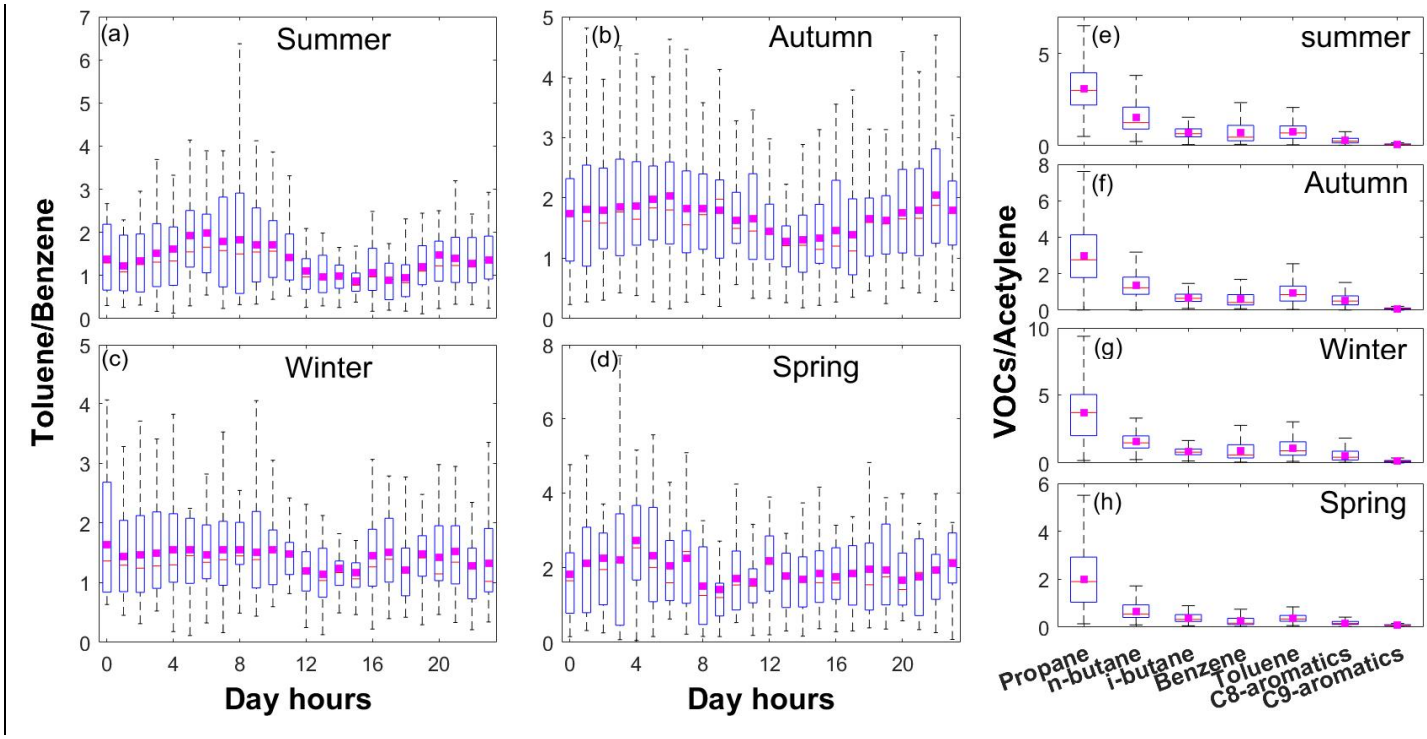

920

~~**Figure 4: Diurnal variations in toluene/benzene ratios (a, b, c, & d) and in the ratios of different VOCs to acetylene in different seasons (e, f, g, & h). The pink-colored squares in the box-plots represent the average values.**~~

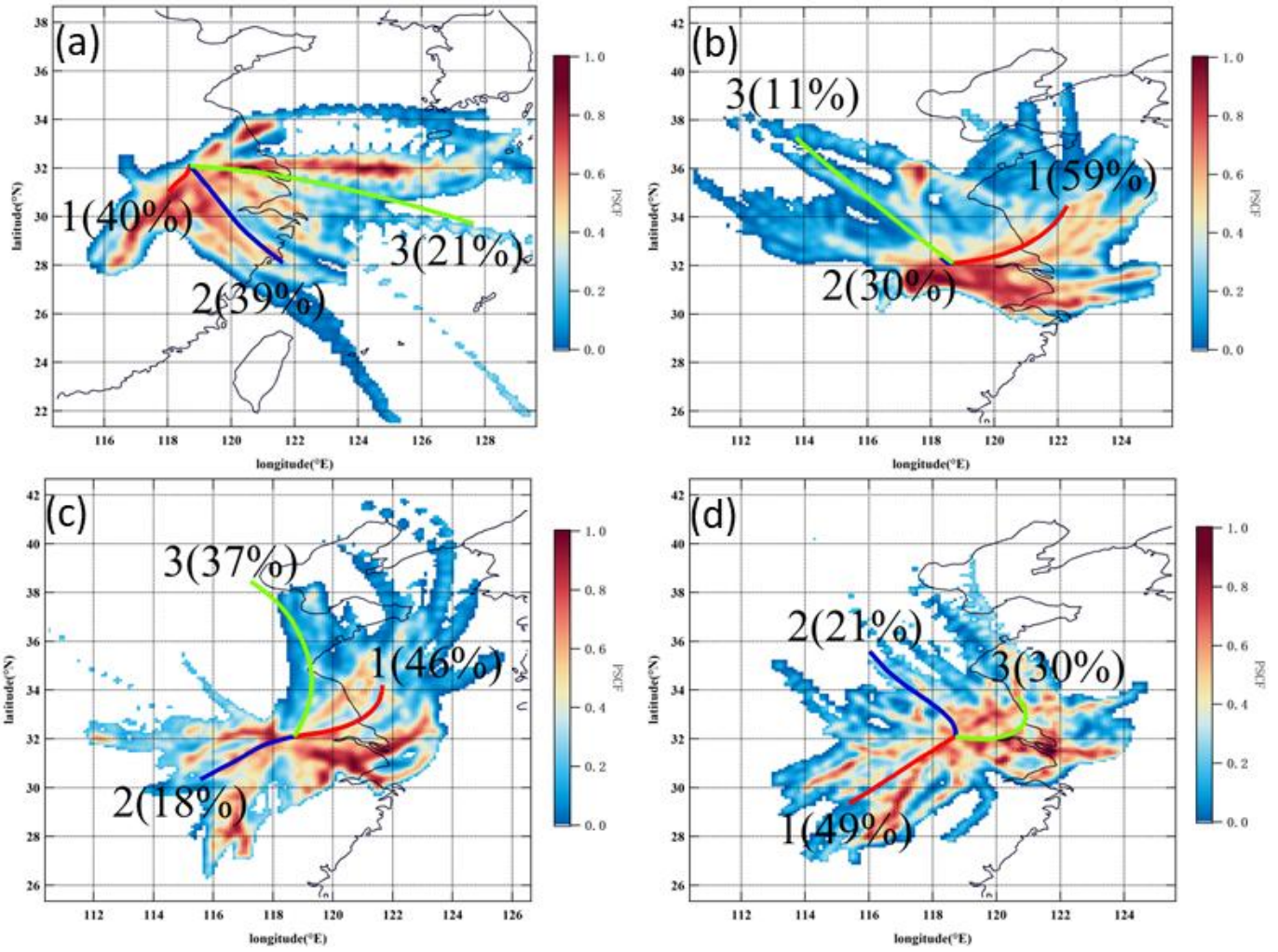

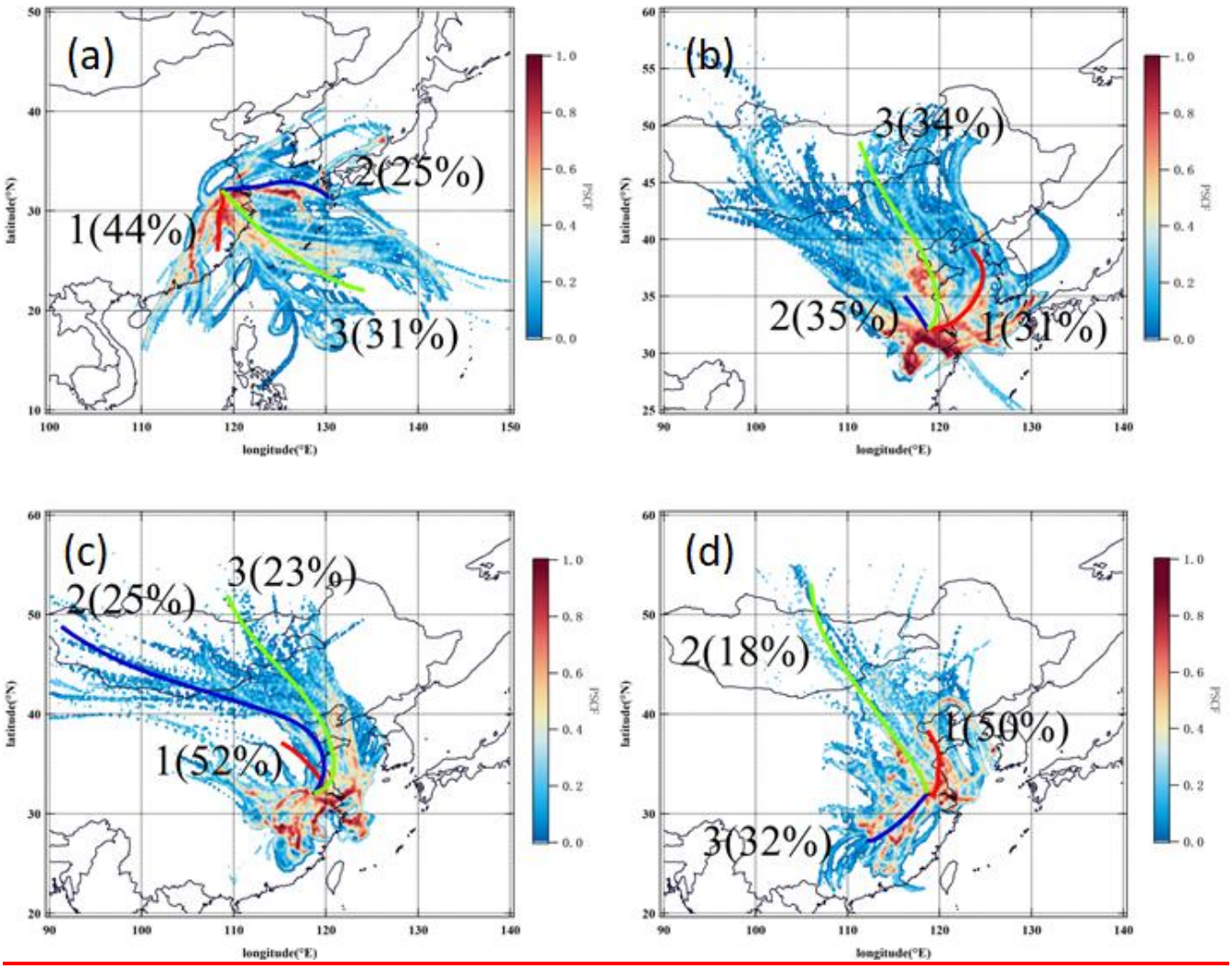

925

Figure 5: Wind cluster and PSCF analysis during (a) summer (b) autumn, (c) winter, and (d) spring based on the ~~24~~ 72 hours backward air mass trajectories from the study area.

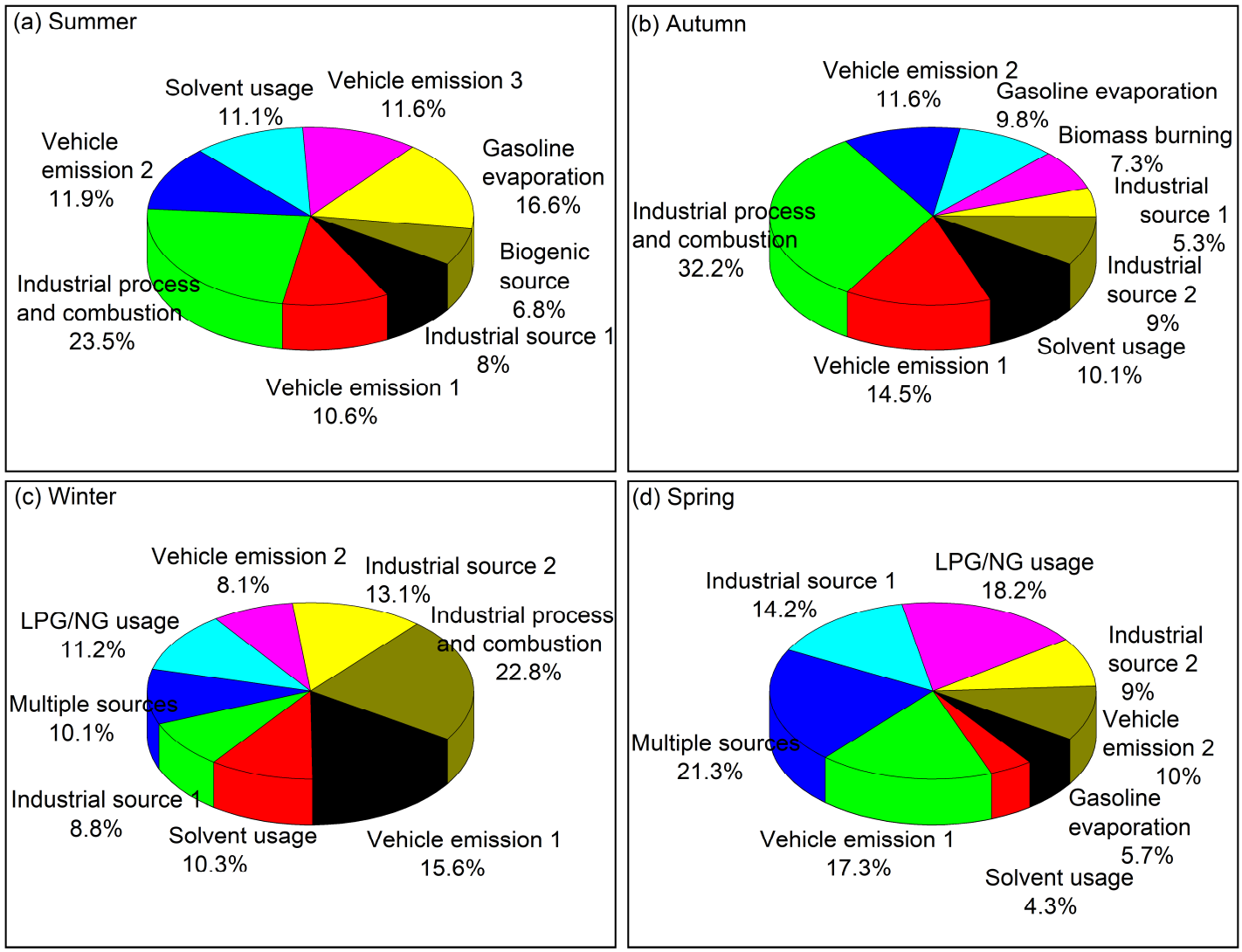
(a) Summer
Solvent usage 11.1%
Vehicle emission 3 11.6%
Vehicle emission 2 11.9%
Gasoline evaporation 16.6%
Biogenic source 6.8%
Industrial process and combustion 23.5%
Industrial source 1 8%
Vehicle emission 1 10.6%
(b) Autumn
Vehicle emission 2 11.6%
Gasoline evaporation 9.8%
Biomass burning 7.3%
Industrial source 1 5.3%
Industrial process and combustion 32.2%
Industrial source 2 9%
Solvent usage 10.1%
Vehicle emission 1 14.5%
(c) Winter
Vehicle emission 2 8.1%
Industrial source 2 13.1%
LPG/NG usage 11.2%
Industrial process and combustion 22.8%
Multiple sources 10.1%
Industrial source 1 8.8%
Solvent usage 10.3%
Vehicle emission 1 15.6%
(d) Spring
Industrial source 1 14.2%
LPG/NG usage 18.2%
Industrial source 2 9%
Vehicle emission 2 10%
Multiple sources 21.3%
Gasoline evaporation 5.7%
Vehicle emission 1 17.3%
Solvent usage 4.3%

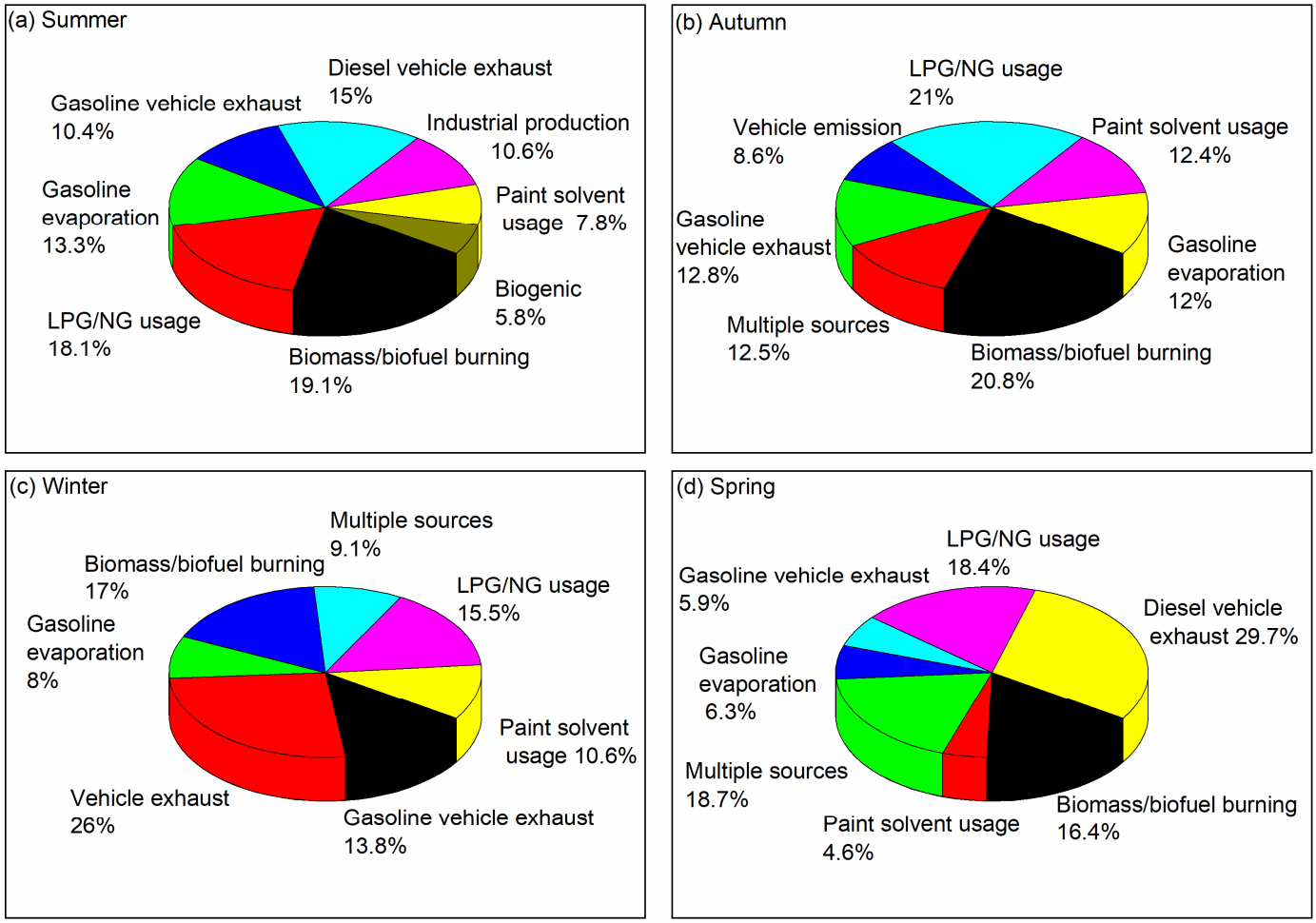

930 **Figure 6: relative contributions of different sources to ambient VOCs in Nanjing industrial area during different seasons**

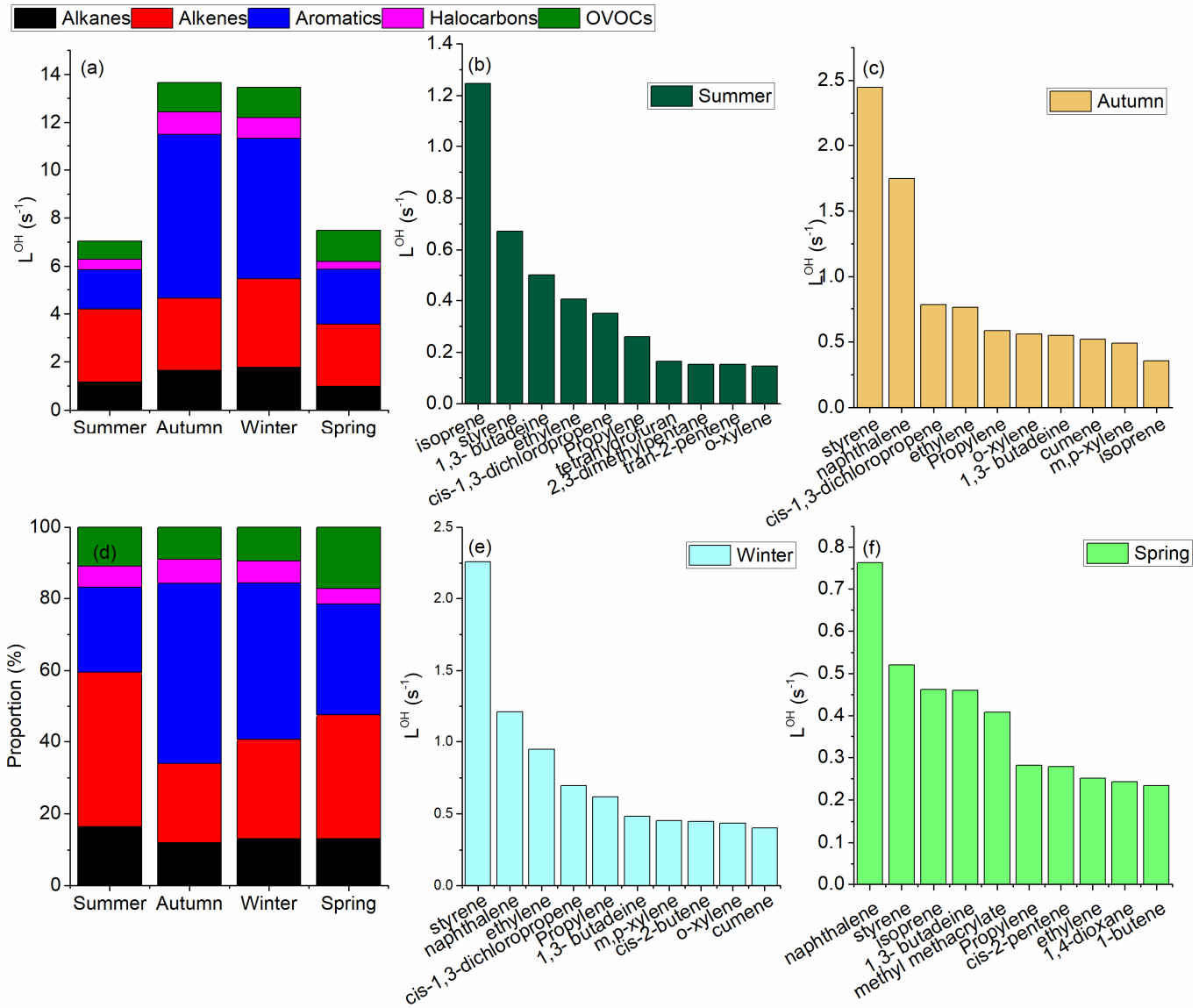

935 **Figure 7: Contribution to OH loss rates of different VOC-groups and the top 10 VOC species in different seasons**

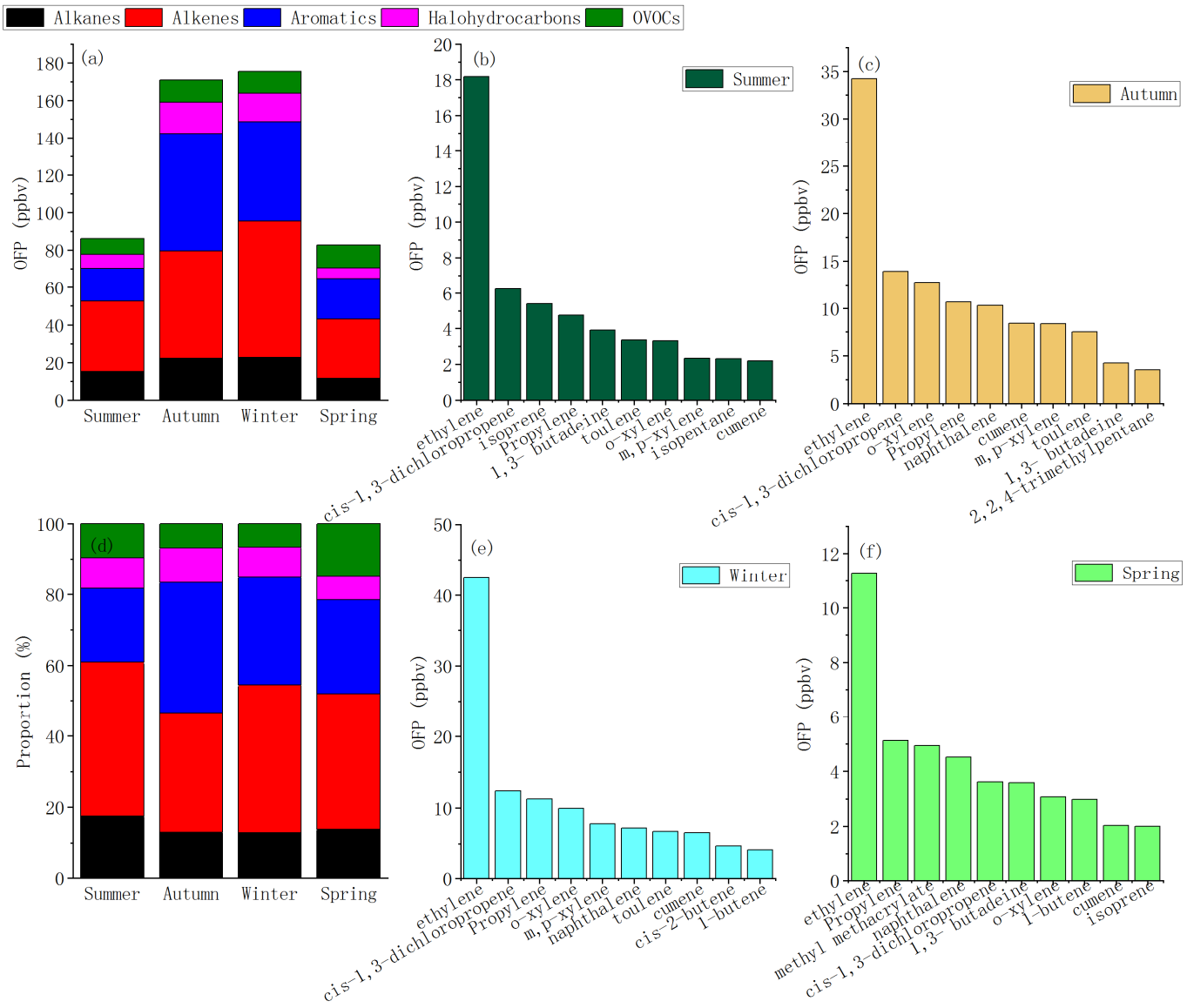

~~Figure 8: Contribution to ozone formation potential of different VOC-groups and the top 10 VOC species in different seasons~~

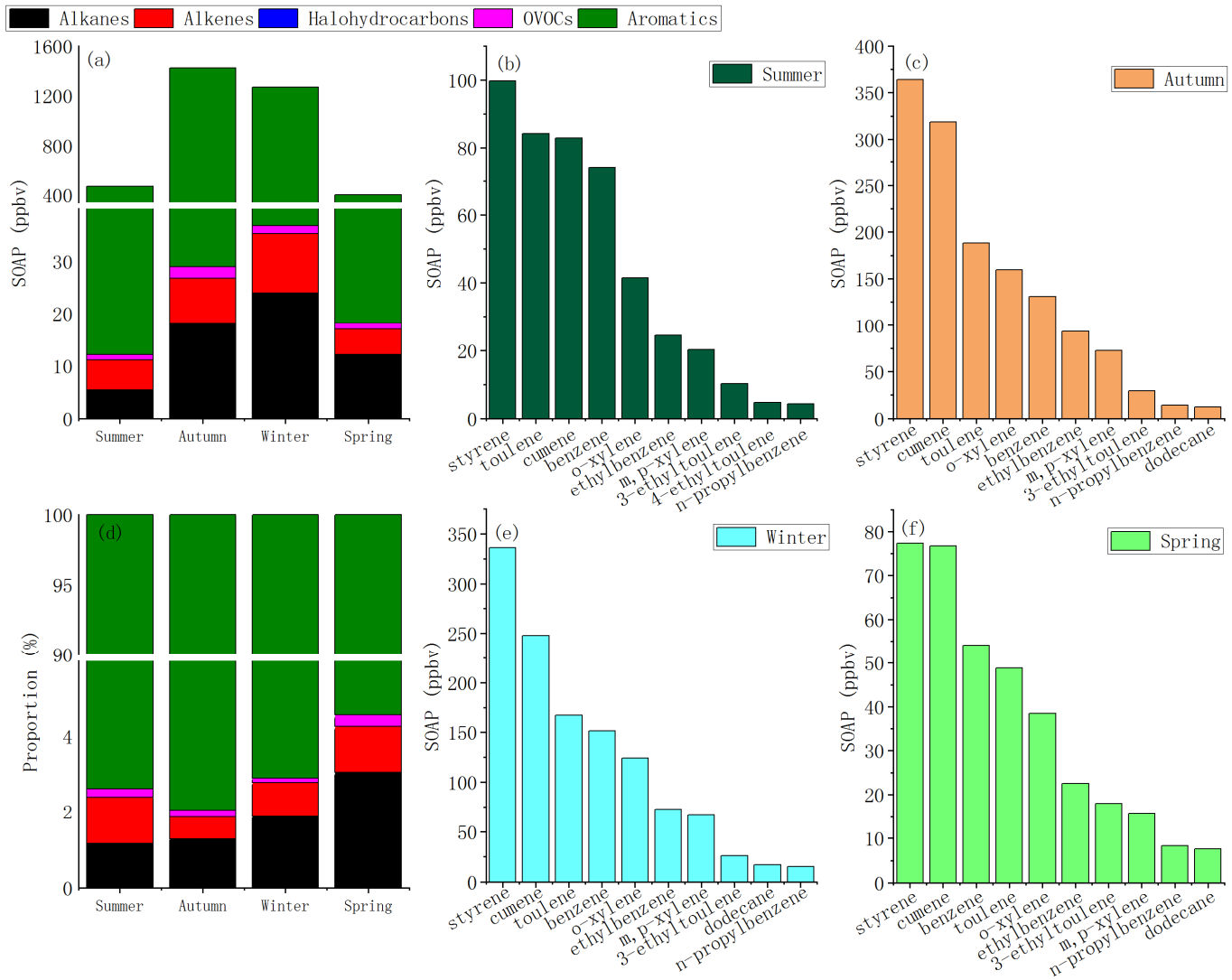

~~Figure 9: Contribution to secondary organic aerosol formation potential of different VOC groups and the top 10 VOC species in different seasons~~

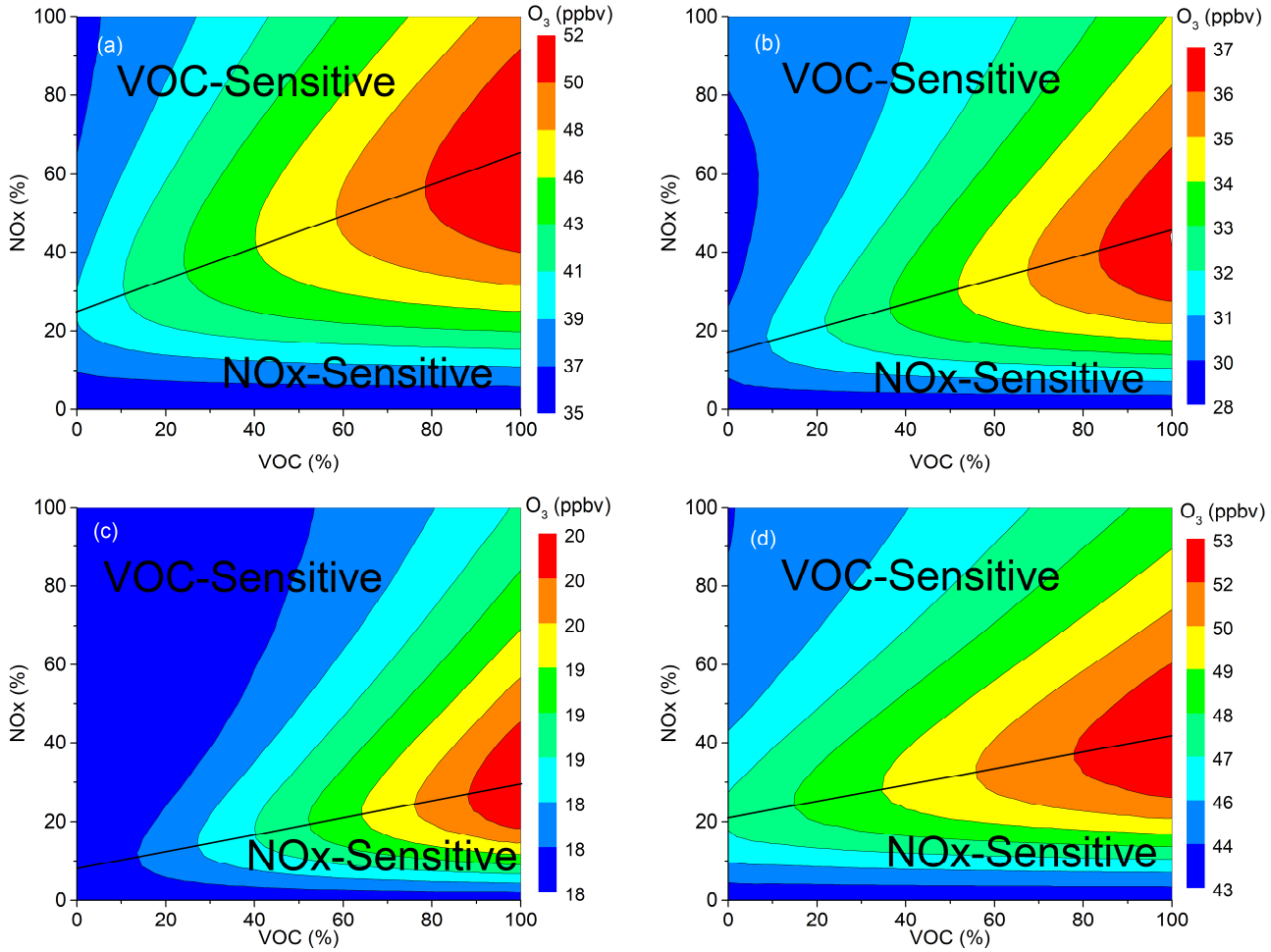

Figure 10: O_3 isopleth diagram for (a) summer (b) autumn, (c) winter, and (d) spring based on percentage changes in VOCs and NOx concentrations in Nanjing and corresponding modelled O_3 production.

950

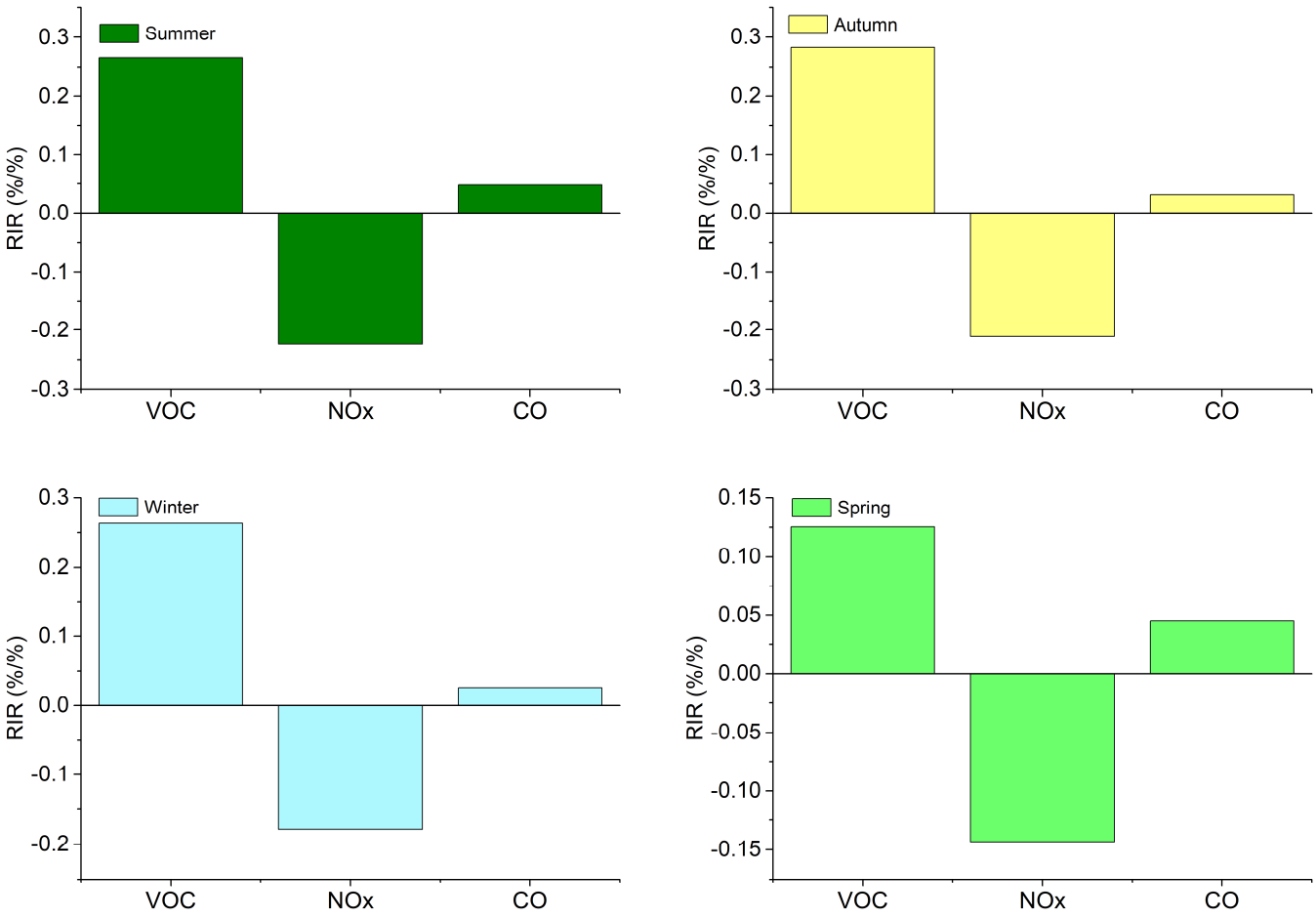

Figure 11: The RIR values of the VOC, NOx, and CO for the different seasons in Nanjing

Measurement report: High Contributions of Halocarbon and Aromatic Compounds to Atmospheric VOCs in Industrial Area

Ahsan Mozaffar [1,2,3], Yan-Lin Zhang [1,2,3*], Yu-Chi Lin[1,2,3], Feng Xie [1,2,3], Mei-Yi Fan [1,2,3], and Fang Cao [1,2,3]

[1]Yale-NUIST Center on Atmospheric Environment, International Joint Laboratory on Climate and Environment Change, Nanjing University of Information Science and Technology, Nanjing, 210044, China.

[2]Key Laboratory Meteorological Disaster; Ministry of Education & Collaborative Innovation Center on Forecast and Evaluation of Meteorological Disaster, Nanjing University of Information Science and Technology, Nanjing, 210044, China.

[3]Jiangsu Provincial Key Laboratory of Agricultural Meteorology, College of Applied Meteorology, Nanjing University of Information Science & Technology, Nanjing 210044, China.

Correspondence to: Yan-Lin Zhang (dryanlinzhang@outlook.com)

Table S1: OH reaction rate constant (K_{OH}) of VOCs and list of VOCs constrained in the F0AM model

Compounds	**K_{OH} (cm^3 $molecule^{-1}$ s^{-1}) (Carter, 2010)**	**Constrained in F0AM model**
Ethane	2.54E-13	Yes
propane	1.11E-12	Yes
isobutane	2.14E-12	Yes
n-butane	2.38E-12	Yes
isopentane	3.60E-12	Yes
n-pentane	3.84E-12	Yes
2,2 dimethylbutane	2.27E-12	
2,3 dimethyl butane	5.79E-12	
2-methyl pentane	5.20E-12	Yes
cyclopentane	5.02E-12	

3-methylpentane	5.20E-12	
n-hexane	5.25E-12	Yes
2,4-dimethylpentane	4.77E-12	
methylcyclopentane	5.68E-12	
isoheptane	6.81E-12	Yes
cyclohexane	7.02E-12	
2,3-dimethylpentane	7.15E-12	
3-methylhexane	7.17E-12	Yes
2,2,4-trimethylpentane	3.38E-12	
heptane	6.81E-12	Yes
methylcyclohexane	9.64E-12	
2-methylheptane	8.31E-12	
n-octane	8.16E-12	Yes
n-nonane	9.75E-12	Yes
Decane	1.10E-11	Yes
n-hendecane	1.23E-11	Yes
dodecane	1.32E-11	Yes
ethylene	8.15E-12	Yes
Propylene	2.60E-11	Yes
trans-2-butene	6.32E-11	Yes
cis-2-butene	5.58E-11	
1-butene	3.11E-11	Yes
1,3- butadeine	6.59E-11	
1-pentene	3.14E-11	Yes
tran-2-pentene	6.70E-11	
isoprene	9.96E-11	Yes
cis-2-pentene	6.50E-11	Yes
1-hexene	3.70E-11	Yes
acetylene	7.56E-13	Yes
benzene	1.22E-12	Yes
toluene	5.58E-12	Yes

ethylbenzene	7.00E-12	Yes
m,p-xylene	2.31E-11	Yes
o-xylene	1.36E-11	Yes
Styrene	5.80E-11	Yes
Cumene	6.30E-12	Yes
n-propylbenzene	5.80E-12	Yes
3-ethyltoulene	1.86E-11	Yes
4-ethyltoulene	1.18E-11	Yes
Mesitylene	5.67E-11	Yes
2-ethyltoulene	1.19E-11	Yes
1,2,4-trimethylbenzene	3.25E-11	Yes
1,2,3-trimethylbenzene	3.27E-11	Yes
1,3-diethylbenzene	2.55E-11	
1,4-diethylbenzene	1.64E-11	Yes
Naphthalene	2.30E-11	
Chloromethane	4.48E-14	Yes
vinyl chloride	6.90E-12	Yes
methyl bromide	4.12E-14	
Chloroethene	0	Yes
trichlorofloromethane	0	
Vinylidene chloride	0	
1,1,2-Trichlor-1,2,2-trifluorethan	0	
Dichloromethane	1.45E-13	Yes
trans-1,2-dichloroethylene	0	
1,1-dichloroethane	2.60E-13	Yes
cis-1,2-dichloroethylene	0	
Chloroform	1.06E-13	Yes
carbon tetrachloride	0	
1,2-dichloroethane	2.53E-13	Yes

Trichloroethylene	2.34E-12	Yes
1,2-dichloropropane	4.50E-13	Yes
bromodichloromethane	0	
trans-1,3-dichloropropene	1.44E-11	
cis-1,3-dichloropropene	8.45E-12	
1,1,2-trichloroethane	2.00E-13	Yes
tetrachloroethylene	0	Yes
1,2-dibromoethane	2.27E-13	Yes
Chlorobenzene	7.70E-13	
Bromoform	0	
1,1,2,2-tetrachloroethane	0	Yes
1,3-dichlorobenzene	5.55E-13	
1,4 dichlorobebezne	5.55E-13	
benzyl chloride	0	
1,2-dichlorobenzene	5.55E-13	
1,2,4-trichlorobenzene	0	
hexachloro-1,3-butadiene	0	
carbon disulfide	2.76E-12	
Acrolein	1.99E-11	Yes
Acetone	1.91E-13	Yes
Isopropanol	5.09E-12	Yes
MTBE	0	Yes
vinyl acetate	3.16E-11	
MEK	1.20E-12	Yes
ethyl acetate	1.60E-12	Yes
Tetrahydrofuran	1.61E-11	
methyl methacrylate	5.25E-11	
1,4-dioxane	3.83E-11	
4-methyl-2-pentanone	1.27E-11	Yes
2-hexanone	9.10E-12	Yes

Table S2: VOC concentrations (ppbv) measured in the industrial area in Nanjing. VOC concentrations observed in previous studies in Nanjing are also listed.

Compounds	Current study										(An et al., 2017), Nanjing		(Wu et al., 2020), Nanjing
	Summer		Autumn		Winter		Spring		Yearly		Summer	Winter	Yearly
	Mean	Std	Mean	Std	Mean	Std	Mean	Std	Mean	Std	Mean	Mean	Mean
ethane	2.81	0.58	8.06	1.77	7.66	1.39	4.76	1.25	5.82	2.49	2.76	7.66	2.89
propane	3.12	0.63	6.09	1.21	4.92	0.91	2.73	0.92	4.22	1.57	1.70	4.51	3.29
isobutane	0.75	0.16	1.25	0.26	1.16	0.15	0.48	0.14	0.91	0.36	1.04	2.25	0.9
n-butane	1.75	0.39	2.61	0.63	2.32	0.26	0.87	0.29	1.89	0.76	1.09	2.35	1.53
isopentane	1.59	0.29	1.56	0.47	1.63	0.31	0.42	0.19	1.30	0.59	0.86	1.13	1.26
n-pentane	0.66	0.17	1.06	0.29	1.36	0.25	0.31	0.10	0.85	0.46	0.50	0.86	0.78
2,2 dimethylbutane	0.08	0.01	0.06	0.01	0.06	0.01	0.06	0.01	0.06	0.01	0.28	0.03	0.04
2,3 dimethyl butane	0.13	0.03	0.18	0.03	0.11	0.00	0.20	0.02	0.16	0.04	0.12	0.35	0.04
2-methyl pentane	0.26	0.08	0.32	0.10	0.44	0.11	0.29	0.06	0.33	0.08	0.25	0.41	0.16
cyclopentane	0.15	0.03	0.10	0.02	0.08	0.01	0.22	0.03	0.14	0.06	0.08	0.12	0.08
3-methylpentane	0.25	0.06	0.38	0.09	0.37	0.12	0.25	0.08	0.31	0.07	0.22	0.31	0.26
n-hexane	0.17	0.04	0.33	0.09	0.41	0.17	0.21	0.06	0.28	0.11	0.41	0.48	0.47
2,4-dimethylpentane	0.06	0.00	0.06	0.01	0.06	0.00	0.13	0.01	0.08	0.03	0.05	0.08	0.01
methylcyclopentane	0.12	0.03	0.16	0.04	0.14	0.04	0.13	0.03	0.14	0.02	0.08	0.13	0.26
isoheptane	0.13	0.04	0.12	0.04	0.11	0.04	0.16	0.03	0.13	0.02			
cyclohexane	0.44	0.29	0.37	0.15	0.43	0.31	0.21	0.13	0.36	0.10	0.41	0.60	0.15
2,3-dimethylpentane	0.86	0.59	0.73	0.30	0.85	0.63	0.42	0.25	0.72	0.21	0.11	0.20	0.02

3-methylhexane	0.10	0.02	0.12	0.03	0.09	0.02	0.14	0.02	0.11	0.02	0.04	0.05	0.08
2,2,4-trimethylpentane	1.59	0.37	2.81	0.82	3.26	0.78	1.16	0.74	2.21	0.99	0.03	0.02	0.03
heptane	0.10	0.01	0.12	0.02	0.12	0.01	0.10	0.01	0.11	0.01	1.92	0.2	0.11
methylcyclohexane	0.18	0.02	0.18	0.04	0.19	0.03	0.16	0.03	0.18	0.01	0.08	0.12	0.08
2-methylheptane	0.08	0.00	0.08	0.01	0.08	0.00	0.17	0.01	0.10	0.04	0.01	0.05	0.02
n-octane	0.09	0.01	0.08	0.01	0.09	0.01	0.20	0.01	0.11	0.06	0.19	0.21	0.05
n-noane	0.06	0.00	0.08	0.02	0.08	0.02	0.07	0.00	0.07	0.01	0.03	0.05	0.03
decane	0.05	0.00	0.06	0.01	0.06	0.01	0.05	0.00	0.06	0.01	0.05	0.06	0.04
n-hendecane	0.04	0.01	0.16	0.01	0.22	0.01	0.17	0.01	0.15	0.07	0.06	0.09	0.02
dodecane	0.08	0.00	0.36	0.02	0.50	0.01	0.22	0.02	0.29	0.18	0.07	0.13	0.03
ethylene	2.02	0.58	3.80	0.89	4.71	1.09	1.25	0.71	2.95	1.59	3.08	6.62	1.21
Propylene	0.41	0.34	0.91	0.46	0.97	0.31	0.44	0.58	0.68	0.30	0.98	2.09	0.70
trans-2-butene	0.02	0.00	0.06	0.02	0.23	0.01	0.03	0.01	0.09	0.10	0.07	0.14	0.07
cis-2-butene	0.07	0.00	0.16	0.03	0.33	0.03	0.09	0.01	0.16	0.12	0.06	0.10	0.05
1-butene	0.07	0.00	0.10	0.02	0.43	0.02	0.31	0.13	0.22	0.17	0.18	0.23	0.15
1,3- butadeine	0.31	0.07	0.34	0.05	0.30	0.03	0.28	0.00	0.31	0.02			
1-pentene	0.16	0.03	0.14	0.03	0.08	0.03	0.10	0.03	0.12	0.04	0.04	0.05	0.04
tran-2-pentene	0.09	0.03	0.06	0.02	0.05	0.01	0.09	0.02	0.07	0.02	0.03	0.04	0.03
isoprene	0.51	0.37	0.15	0.06	0.09	0.02	0.19	0.02	0.23	0.19	0.58	0.07	0.18
cis-pentene	0.07	0.02	0.06	0.01	0.07	0.01	0.17	0.02	0.09	0.05	0.03	0.02	0.02
1-hexene	0.05	0.03	0.06	0.02	0.06	0.03	0.24	0.01	0.10	0.09	0.03	0.02	0.01
acetylene	1.02	0.15	1.77	0.24	1.59	0.15	1.20	0.13	1.40	0.35	2.63	6.46	
benzene	0.80	0.19	1.41	0.41	1.63	0.39	0.58	0.37	1.10	0.50	1.86	3.21	0.82
toulene	0.84	0.40	1.88	0.51	1.67	0.31	0.49	0.12	1.22	0.66	1.47	3.20	1.07
ethylbenzene	0.22	0.05	0.83	0.21	0.65	0.15	0.20	0.10	0.48	0.32	1.27	1.79	0.43
m,p-xylene	0.24	0.07	0.86	0.24	0.80	0.17	0.19	0.07	0.52	0.36	0.46	0.59	0.67
o-xylene	0.43	0.09	1.67	0.42	1.30	0.29	0.40	0.21	0.95	0.63	0.28	0.39	0.21
styrene	0.47	0.15	1.71	0.49	1.58	0.35	0.36	0.15	1.03	0.71	0.17	0.30	0.12

cumene	0.87	0.19	3.34	0.84	2.60	0.59	0.80	0.41	1.90	1.27			
n-propylbenzene	0.04	0.01	0.13	0.02	0.14	0.01	0.08	0.11	0.10	0.05	0.09	0.08	0.03
3-ethyltoulene	0.10	0.02	0.29	0.06	0.26	0.05	0.18	0.21	0.21	0.09	0.05	0.05	0.03
4-ethyltoulene	0.07	0.00	0.08	0.01	0.08	0.01	0.10	0.06	0.08	0.01	0.19	0.29	0.03
mesitylene	0.03	0.00	0.06	0.02	0.08	0.03	0.04	0.00	0.05	0.02			
2-ethyltoulene	0.04	0.01	0.07	0.02	0.07	0.02	0.06	0.07	0.06	0.02	0.51	0.08	
1,2,4-trimethylbenzene	0.06	0.01	0.06	0.02	0.08	0.03	0.13	0.11	0.08	0.03	0.33	0.42	0.09
1,2,3-trimethylbenzene	0.08	0.01	0.20	0.03	0.22	0.01	0.10	0.01	0.15	0.07	0.05	0.05	0.05
1,3-diethylbenzene	0.09	0.00	0.18	0.02	0.17	0.01	0.16	0.01	0.15	0.04	0.03	0.05	0.01
1,4-diethylbenzene	0.09	0.00	0.17	0.02	0.20	0.01	0.17	0.01	0.16	0.05	0.04	0.10	0.04
naphthalene	0.13	0.02	3.09	0.98	2.14	0.22	1.35	0.29	1.68	1.25			
chloromethane	0.16	0.02	0.56	0.08	1.21	0.33	0.15	0.01	0.52	0.50			
vinyl chloride	0.05	0.00	0.07	0.02	0.09	0.02	0.16	0.01	0.09	0.05			
methyl briomide	0.04	0.00	0.05	0.01	0.04	0.01	0.03	0.00	0.04	0.01			
chloroethene	0.08	0.01	0.08	0.02	0.10	0.03	0.05	0.01	0.08	0.02			
trichloroflorome thane	0.23	0.01	0.18	0.01	0.30	0.02	0.21	0.04	0.23	0.05			
Vinylidene chloride	0.05	0.01	0.05	0.01	0.04	0.00	0.05	0.01	0.05	0.00			
1,1,2-Trichlor-1,2,2-trifluorethan	0.08	0.00	0.08	0.01	0.10	0.00	0.08	0.01	0.08	0.01			
dichloromethane	1.26	0.09	3.09	0.54	2.62	0.47	1.97	0.53	2.23	0.80			
trans-1,2-	0.05	0.00	0.05	0.01	0.05	0.01	0.14	0.01	0.07	0.05			

dichloroethylene										
1,1-dichloroethane	0.33	0.08	0.65	0.18	0.82	0.34	0.41	0.13	0.55	0.22
cis-1,2-dichloroethylene	0.07	0.00	0.07	0.01	0.03	0.00	0.20	0.01	0.09	0.07
chloroform	0.17	0.02	0.57	0.16	0.53	0.18	0.18	0.04	0.36	0.22
carbon tetrachloride	0.12	0.01	0.18	0.02	0.17	0.03	0.18	0.02	0.16	0.03
1,2-dichloroethane	0.95	0.14	3.19	0.40	2.95	0.43	1.15	0.31	2.06	1.17
trichloroethylene	0.13	0.02	0.14	0.02	0.10	0.02	0.06	0.00	0.11	0.04
1,2-dichloropropane	0.57	0.21	1.48	0.53	0.96	0.23	0.14	0.05	0.79	0.57
bromodichloromethane	0.06	0.00	0.03	0.01	0.03	0.00	0.06	0.00	0.04	0.01
trans-1,3-dichloropropene	0.10	0.00	0.08	0.01	0.13	0.00	0.17	0.01	0.12	0.04
cis-1,3-dichloropropene	1.68	0.79	3.76	1.02	3.35	0.62	0.98	0.23	2.44	1.33
1,1,2-trichloroethane	0.06	0.01	0.12	0.04	0.11	0.07	0.05	0.05	0.09	0.03
tetrachloroethylene	0.06	0.00	0.09	0.02	0.08	0.02	0.06	0.01	0.07	0.01
1,2-dibromoethane	0.03	0.00	0.02	0.01	0.02	0.00	0.02	0.00	0.02	0.01
chlorobenzene	0.31	0.18	1.89	0.91	1.73	1.14	0.20	0.16	1.03	0.90
bromoform	0.02	0.00	0.02	0.01	0.02	0.00	0.02	0.00	0.02	0.00
1,1,2,2-tetrachloroethane	0.94	0.30	3.43	0.97	3.16	0.70	0.73	0.30	2.06	1.43

1,3-dichlorobenzene	0.02	0.00	0.09	0.03	0.14	0.05	0.04	0.01	0.07	0.05
1,4 dichlorobebezne	0.11	0.01	0.65	0.20	0.40	0.05	0.09	0.01	0.31	0.27
benzyl chloride	0.12	0.02	0.10	0.05	0.13	0.07	0.24	0.23	0.15	0.06
1,2-dichlorobenzene	0.03	0.01	0.25	0.11	0.15	0.04	0.08	0.01	0.13	0.10
1,2,4-trichlorobenzene	0.04	0.00	0.17	0.04	0.25	0.01	0.14	0.02	0.15	0.09
hexachloro-1,3-butadiene	0.02	0.00	0.17	0.04	0.15	0.04	0.02	0.00	0.09	0.08
carbon disulfide	0.42	0.11	0.59	0.13	0.66	0.15	0.21	0.07	0.47	0.20
Acrolein	0.09	0.02	0.07	0.02	0.05	0.01	0.07	0.02	0.07	0.01
acetone	1.60	0.29	2.98	0.25	1.94	0.22	2.61	0.61	2.28	0.63
isopropanol	0.46	0.07	2.34	0.60	1.28	0.34	0.44	0.10	1.13	0.90
MTBE	0.37	0.11	0.66	0.23	0.35	0.11	0.35	0.13	0.43	0.15
vinyl acetate	0.17	0.04	0.33	0.09	0.42	0.18	0.26	0.08	0.30	0.11
MEK	0.69	0.06	1.14	0.10	0.73	0.09	0.77	0.43	0.84	0.21
ethyl acetate	1.06	0.17	1.56	0.25	1.43	0.18	1.34	0.95	1.35	0.21
tetrahydrofuran	0.41	0.56	0.08	0.11	0.43	0.45	0.24	0.03	0.29	0.16
methyl methacrylate	0.11	0.01	0.21	0.01	0.20	0.01	0.32	0.00	0.21	0.09
1,4-dioxane	0.05	0.00	0.07	0.01	0.09	0.00	0.26	0.01	0.12	0.10
4-methyl-2-pentanone	0.23	0.08	0.31	0.07	0.28	0.06	0.30	0.03	0.28	0.03
2-hexanone	0.15	0.00	0.23	0.01	0.28	0.01	0.29	0.02	0.23	0.07
TVOC	**38.81**	**10.21**	**83.05**	**20.07**	**77.51**	**16.77**	**39.62**	**13.12**	**59.75**	**28.57**

S1. Source apportionment of VOCs

Figure S1 shows the source profile of summertime VOCs obtained from the PMF model. The resolved factors were identified as biomass/biofuel burning, LPG/NG usage, gasoline evaporation, gasoline vehicle exhaust, diesel vehicle exhaust, industrial production, paint solvent usage, and biogenic source. Factor 1 was characterized by high concentrations of ethane and ethylene. These compounds are tracers of incomplete combustion which emitted from vehicle exhaust and biomass/biofuel burning (An et al., 2017). Benzene, toluene, pentane, and decane concentrations were low in factor 1, therefore, it was identified as biomass/biofuel burning. Factor 2 was distinguished by a significant presence of LPG/NG VOCs propane, isobutene, and n-butane (Shao et al., 2016). So, factor 2 was identified as LPG/NG usage. Factor 3 was dominated by high concentrations of isopentane, n-pentane, and MTBE. Therefore, factor 3 was identified as gasoline evaporation (Song et al., 2018; Wang et al., 2016). Factor 4 possessed high concentrations of vehicle exhaust VOCs benzene and toluene (Song et al., 2018). Although these VOCs are also emitted by industrial processes, the contribution of benzene was several folds higher than toluene in this factor. Therefore, factor 4 was related to vehicle exhaust emission and it was assigned to gasoline vehicle exhaust (An et al., 2017). Factor 5 was characterized by high concentrations of acetylene, n-heptane, and decane. These are related to vehicle emission, especially diesel vehicle exhaust emission as diesel engine produce more acetylene than the gasoline engine does (Song et al., 2018; An et al., 2017). Therefore, factor 5 was attributed to diesel vehicle exhaust. Factor 6 was dominated by toluene and the sampling site was beside an industrial area. So, we identified this factor as industrial production. Due to the high contribution of o-xylene, m,p-xylene, ethylbenzene and styrene, factor 7 was assigned to paint solvent usage sources (Li et al., 2018). Factor 8 was attributed to the biogenic source, which was mainly distinguished by a high concentration of isoprene (Song et al., 2018).

During autumn, the possible VOC sources were biomass/biofuel burning, multiple sources, gasoline vehicle exhaust, vehicle emission, LPG/NG usage, paint solvent usage and gasoline evaporation (Fig.S2). Factor 1 was represented by a high concentration of ethane and ethylene, so, it was identified as biomass/biofuel burning (An et al., 2017). Factor 2 was dominated by isoprene, n-heptane, decane, and acetylene. Among these compounds isoprene is mainly emitted by trees and rest of the compounds are related to diesel vehicle exhaust emission. Therefore, Factor 2 was identified as multiple sources. Factor 3 was identified as gasoline vehicle exhaust

due to high contribution of benzene and toluene. In factor 3, benzene was several folds higher than toluene. The 4th factor was mainly composed of vehicle emission related compounds 2-methyl pentane, n-hexane, n-heptane, n-pentane, and isopentane, therefore, identified as vehicle emission (Song et al., 2018). Factor 5 was assigned to LPG/NG usage as propane, isobutene, and n-butane were the main contributor to it (Shao et al., 2016). Factor 6 was characterized by a high concentration of o-xylene, m,p-xylene, ethylbenzene and styrene, which are typical tracer of paint solvent usage. Factor 7 was identified as gasoline evaporation, it was dominated by high concentrations of isopentane, n-pentane, and MTBE (Song et al., 2018).

During winter, the source factors were identified as gasoline vehicle exhaust, vehicle exhaust, gasoline evaporation, biomass/biofuel burning, multiple sources, LPG/NG usage, and paint solvent usage (Fig. S3). Factor 1 was assigned to gasoline vehicle exhaust; it was dominated by benzene and toluene and contribution of benzene was twice of toluene. Factor 2 was represented by a high concentration of isobutene, n-butane, acetylene, ethylene, ethane, n-heptane and decane. Isobutene and n-butane are related to LPG/NG usage, but, the contribution of propane was zero in factor 2. Acetylene, ethylene, and ethane emitted from combustion sources like vehicle exhaust and biomass burning. Decane and n-heptane are related to vehicle emission. By considering above information, factor 2 was identified as vehicle exhaust. Factor 3 was identified as gasoline evaporation and it was characterized by high concentrations of isopentane and n-pentane. Factor 4 was characterized by high contribution of ethylene and ethane; therefore, it was identified as biomass/biofuel burning. Factor 5 was characterized by high concentrations of isoprene, propane, n-hexane and n-heptane. Propane is related to LPG/NG usage, isoprene mainly emitted from trees (evergreen trees in winter), and n-hexane and n-heptane are related to vehicle emission. By considering above information, factor 5 was assigned to multiple sources. Factor 6 was dominated by high concentrations of propane. Therefore, it was identified as LPG/NG usage. Factor 7 was identified as paint solvent usage due to the high contribution of o-xylene, m,p-xylene, ethylbenzene and styrene (Zhang et al., 2018; Song et al., 2020).

During spring, the possible VOC sources were biomass/biofuel burning, paint solvent usage, multiple sources, gasoline evaporation, gasoline vehicle exhaust, LPG/NG usage, and diesel vehicle exhaust (Fig. S4). Factors 1 was identified as a biomass/biofuel burning source for the high loading of ethylene and ethane and relatively lower contribution from the vehicle emission related compounds. Due to the high contribution of o-xylene, styrene, m,p-xylene, and

ethylbenzene, factor 2 was assigned to paint solvent usage sources (Li et al., 2018). Factor 3 had a high contribution of isoprene, n-hexane, n-heptane, decane, MTBE, toluene, ethylbenzene, and o-xylene. Therefore, factor 3 was identified as multiple sources. Factor 4 was represented by a high concentration of isopentane, n-pentane, and MTBE. Therefore, factor 4 was identified as gasoline evaporation. Factor 5 was represented by high concentrations of benzene, therefore, identified as gasoline vehicle exhaust. Factor 6 was assigned to LPG/NG usage due to the high contribution of propane, n-butane, and isobutane (Shao et al., 2016). Factor 7 was identified as diesel vehicle exhaust due to the high contribution of acetylene, n-heptane, and decane.

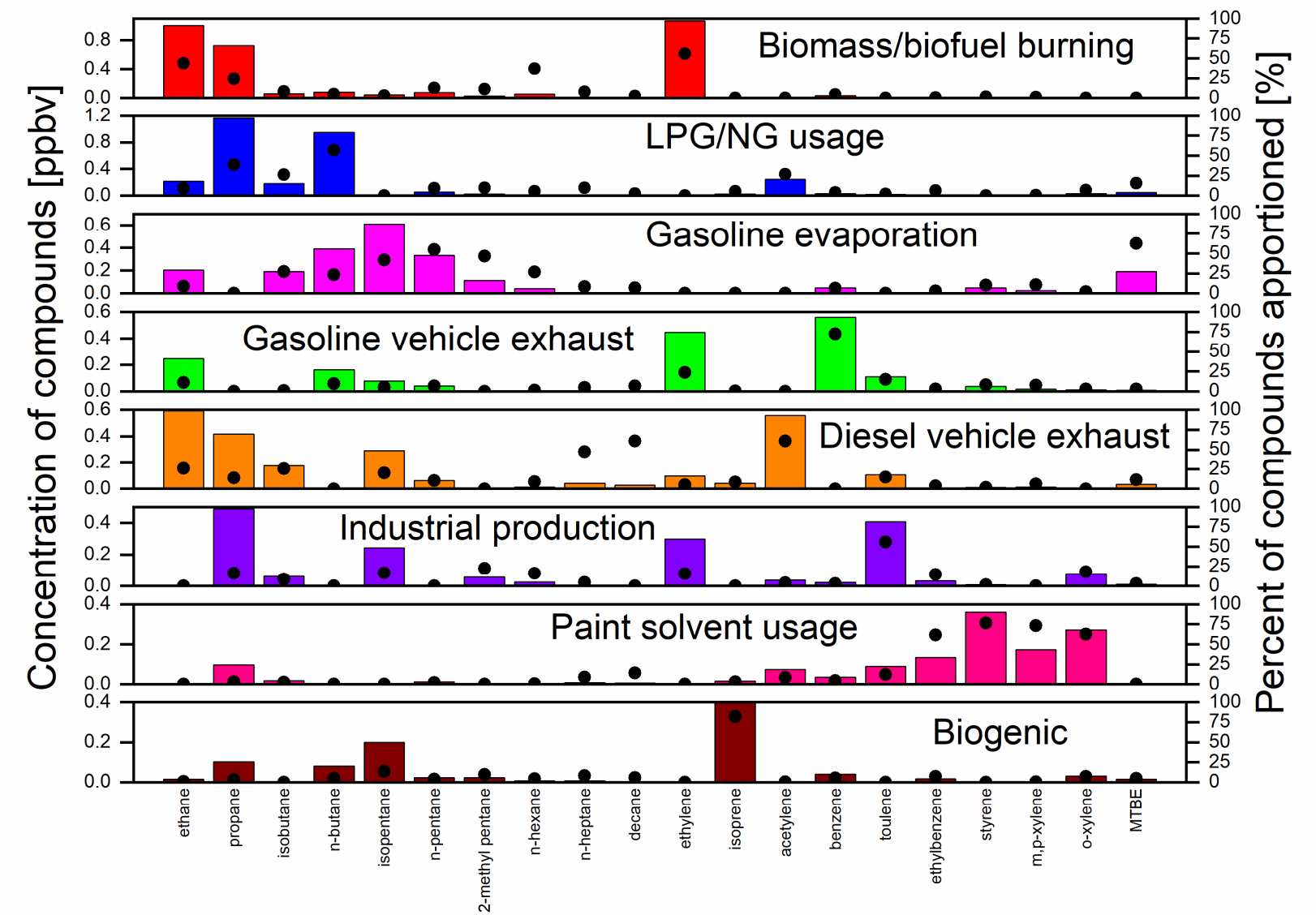

Figure S1: Source profile of VOCs during summer in Nanjing industrial area. Bars and dots represent the concentrations and percentages of the compounds, respectively.

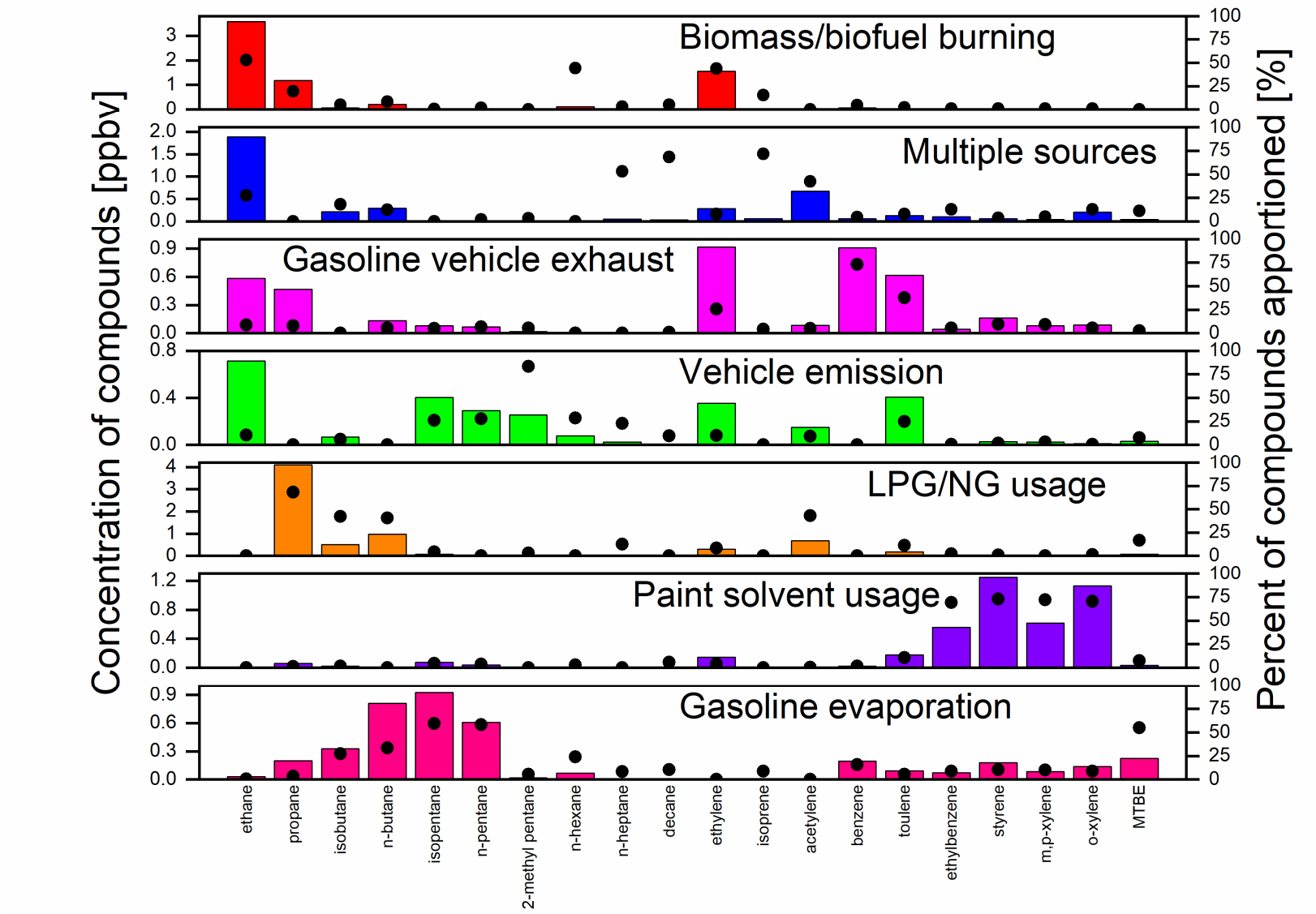

1058

1059 **Figure S2: Source profile of VOCs during autumn in Nanjing industrial area. Bars and dots represent the concentrations and**

1060 **percentages of the compounds, respectively.**

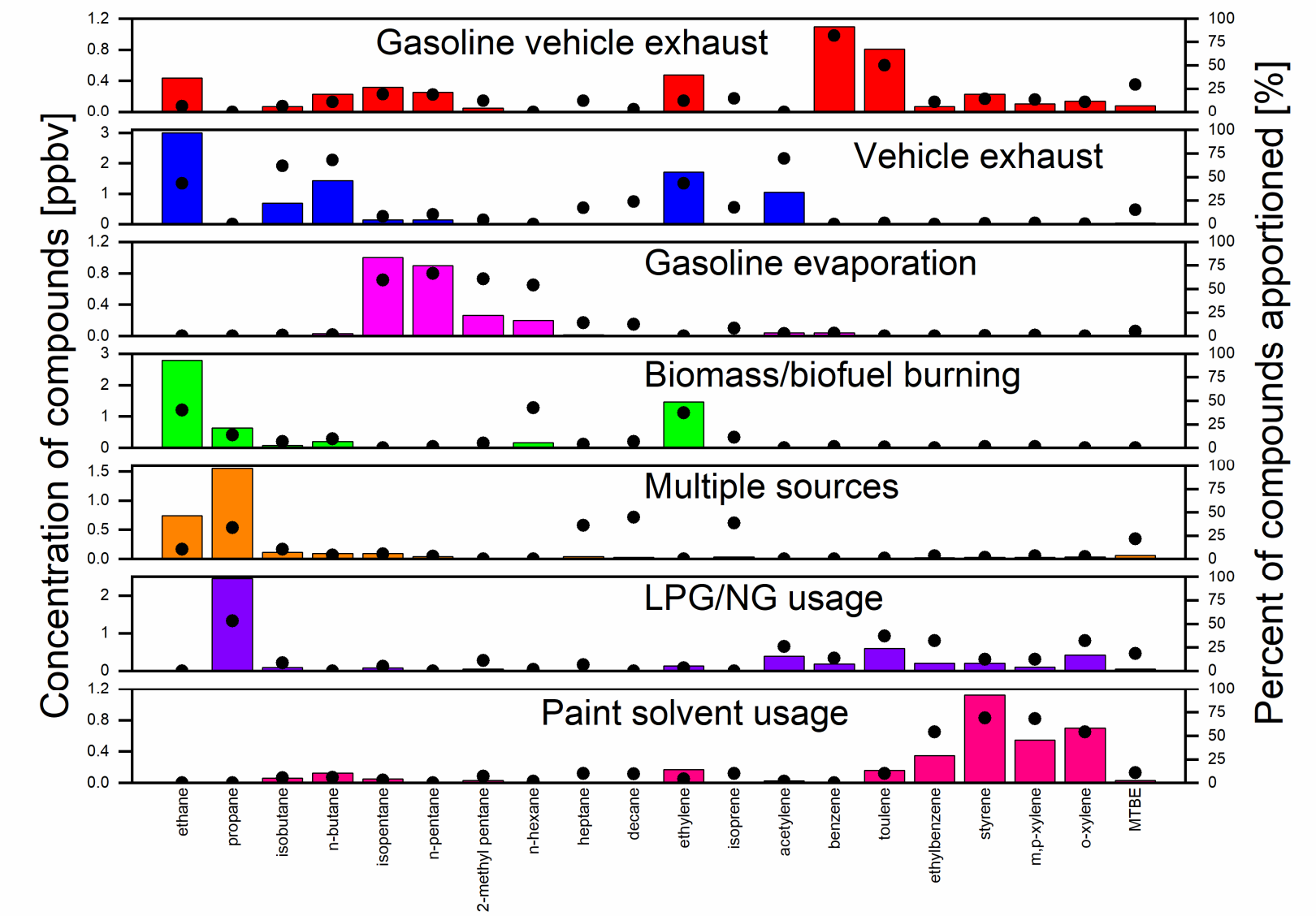

1061

1062 **Figure S3: Source profile of VOCs during winter in Nanjing industrial area. Bars and dots represent the concentrations and**

1063 **percentages of the compounds, respectively.**

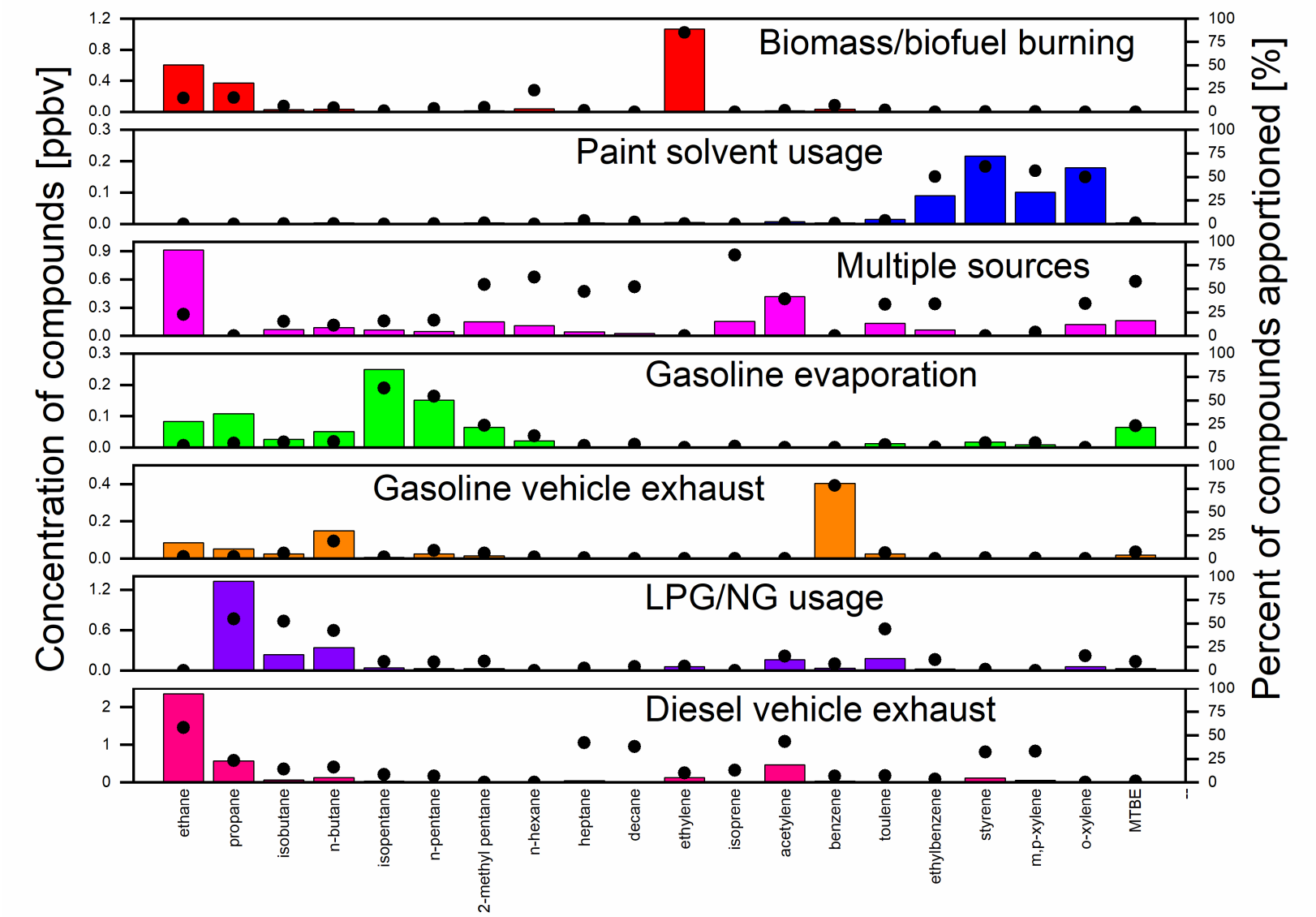

1064

1065 **Figure S4: Source profile of VOCs during spring in Nanjing industrial area. Bars and dots represent the concentrations and**

1066 **percentages of the compounds, respectively.**

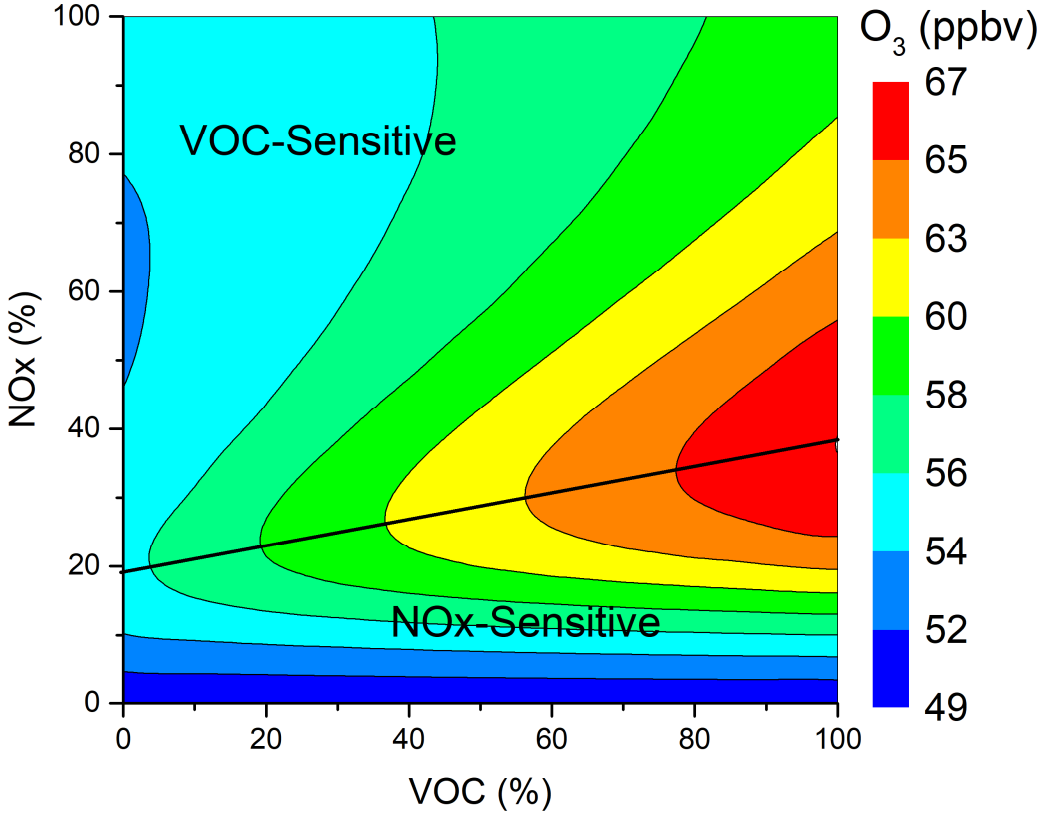

Figure S5: O_3 isopleth diagram on a high O_3 episode day (July 29 2018) in Nanjing industrial area.

References

An, J., Wang, J., Zhang, Y., & Zhu, B. (2017). Source Apportionment of Volatile Organic Compounds in an Urban Environment at the Yangtze River Delta, China. *Archives of Environmental Contamination and Toxicology*, *72*(3), 335–348. https://doi.org/10.1007/s00244-017-0371-3

An, J., Zhu, B., Wang, H., Li, Y., Lin, X., & Yang, H. (2014). Characteristics and source apportionment of VOCs measured in an industrial area of Nanjing, Yangtze River Delta, China. *Atmospheric Environment*, *97*, 206–214. https://doi.org/https://doi.org/10.1016/j.atmosenv.2014.08.021

Borbon, A., Locoge, N., Veillerot, M., Galloo, J. C., & Guillermo, R. (2002). Characterisation of NMHCs in a French urban atmosphere: overview of the main sources. *Science of The Total Environment*, *292*(3), 177–191. https://doi.org/https://doi.org/10.1016/S0048-9697(01)01106-8

Carter, W. P. L. (2010). Development of the SAPRC-07 chemical mechanism. *Atmospheric Environment*, *44*(40), 5324–5335. https://doi.org/10.1016/j.atmosenv.2010.01.026

Derwent, R. G., Jenkin, M. E., Utembe, S. R., Shallcross, D. E., Murrells, T. P., & Passant, N. R. (2010). Secondary organic aerosol formation from a large number of reactive man-made organic compounds. *Science of the Total Environment*, *408*(16), 3374–3381. https://doi.org/10.1016/j.scitotenv.2010.04.013

Dörter, M., Odabasi, M., & Yenisoy-Karakaş, S. (2020). Source apportionment of biogenic and anthropogenic VOCs in Bolu plateau. *Science of the Total Environment*, *731*, 1–18. https://doi.org/10.1016/j.scitotenv.2020.139201

Hui, L., Liu, X., Tan, Q., Feng, M., An, J., Qu, Y., … Cheng, N. (2019). VOC characteristics, sources and contributions to SOA formation during haze events in Wuhan, Central China. *Science of the Total Environment*, *650*, 2624–2639. https://doi.org/10.1016/j.scitotenv.2018.10.029

Hui, L., Liu, X., Tan, Q., Feng, M., An, J., Qu, Y., … Jiang, M. (2018). Characteristics, source apportionment and contribution of VOCs to ozone formation in Wuhan, Central China. *Atmospheric Environment*, *192*(August), 55–71. https://doi.org/10.1016/j.atmosenv.2018.08.042

Li, J., Zhai, C., Yu, J., Liu, R., Li, Y., Zeng, L., & Xie, S. (2018). Spatiotemporal variations of ambient volatile organic compounds and their sources in Chongqing, a mountainous megacity in China. *Science of the Total Environment*, *627*, 1442–1452. https://doi.org/10.1016/j.scitotenv.2018.02.010

Liu, P. W. G., Yao, Y. C., Tsai, J. H., Hsu, Y. C., Chang, L. P., & Chang, K. H. (2008). Source impacts by volatile organic compounds in an industrial city of southern Taiwan. *Science of the Total Environment*, *398*(1–3), 154–163. https://doi.org/10.1016/j.scitotenv.2008.02.053

Liu, Y., Shao, M., Fu, L., Lu, S., Zeng, L., & Tang, D. (2008). Source profiles of volatile organic compounds (VOCs) measured in China: Part I. *Atmospheric Environment*, *42*(25), 6247–6260. https://doi.org/https://doi.org/10.1016/j.atmosenv.2008.01.070

Lyu, X., Guo, H., Simpson, I. J., Meinardi, S., Louie, P. K. K., Ling, Z., … Blake, D. R. (2016). Effectiveness of replacing catalytic converters in LPG-fueled vehicles in Hong Kong. *Atmospheric Chemistry and Physics*, *16*(10), 6609–6626. https://doi.org/10.5194/acp-16-6609-2016

McCulloch, A., Aucott, M. L., Benkovitz, C. M., Graedel, T. E., Kleiman, G., Midgley, P. M., & Li, Y.-F. (1999). Global emissions of hydrogen chloride and chloromethane from coal combustion, incineration and industrial activities: Reactive Chlorine Emissions Inventory. *Journal of Geophysical Research: Atmospheres*, *104*(D7), 8391–8403. https://doi.org/https://doi.org/10.1029/1999JD900025

Pallavi, Sinha, B., & Sinha, V. (2019). Source apportionment of volatile organic compounds in the northwest Indo-Gangetic Plain using a positive matrix factorization model. *Atmospheric Chemistry and Physics*, *19*(24), 15467–15482. https://doi.org/10.5194/acp-19-15467-2019

Reimann, S., Calanca, P., & Hofer, P. (2000). The anthropogenic contribution to isoprene concentrations in a rural atmosphere. *Atmospheric Environment*, *34*(1), 109–115. https://doi.org/https://doi.org/10.1016/S1352-2310(99)00285-X

Saeaw, N., & Thepanondh, S. (2015). Source apportionment analysis of airborne VOCs using positive matrix factorization in industrial and urban areas in Thailand. *Atmospheric Pollution Research*, *6*(4), 644–650. https://doi.org/https://doi.org/10.5094/APR.2015.073

Shao, P., An, J., Xin, J., Wu, F., Wang, J., Ji, D., & Wang, Y. (2016). Source apportionment of VOCs and the contribution to photochemical ozone formation during summer in the typical industrial area in the Yangtze River Delta, China. *Atmospheric Research*, *176–177*, 64–74. https://doi.org/10.1016/j.atmosres.2016.02.015

Song, M., Li, X., Yang, S., Yu, X., Zhou, S., Yang, Y., … Zhang, Y. (2020). Spatiotemporal Variation, Sources, and Secondary Transformation Potential of VOCs in Xi'an, China, *30*(August). Retrieved from https://doi.org/10.5194/acp-2020-704

Song, M., Tan, Q., Feng, M., Qu, Y., Liu, X., An, J., & Zhang, Y. (2018). Source Apportionment and Secondary Transformation of Atmospheric Nonmethane Hydrocarbons in Chengdu, Southwest China. *Journal of Geophysical Research: Atmospheres*, *123*(17), 9741–9763. https://doi.org/10.1029/2018JD028479

Wang, G., Cheng, S., Wei, W., Zhou, Y., Yao, S., & Zhang, H. (2016). Characteristics and source apportionment of VOCs in the suburban area of Beijing , China. *Atmospheric Pollution Research*, *7*(4), 711–724. https://doi.org/10.1016/j.apr.2016.03.006

Wu, F., Yu, Y., Sun, J., Zhang, J., Wang, J., Tang, G., & Wang, Y. (2016). Characteristics, source apportionment and reactivity of ambient volatile organic compounds at Dinghu Mountain in Guangdong Province, China. *Science of the Total Environment*, *548–549*, 347–359. https://doi.org/10.1016/j.scitotenv.2015.11.069

Wu, R., Zhao, Y., Zhang, J., & Zhang, L. (2020). Variability and sources of ambient volatile organic compounds based on online measurements in a suburban region of nanjing, eastern China. *Aerosol and Air Quality Research*, *20*(3), 606–619. https://doi.org/10.4209/aaqr.2019.10.0517

Yu, C. H., Zhu, X., & Fan, Z. (2014). Spatial/temporal variations and source apportionment of VOCs monitored at community scale in an urban area. *PloS One*, *9*(4), e95734–e95734. https://doi.org/10.1371/journal.pone.0095734

Zhang, H., Li, H., Zhang, Q., Zhang, Y., Zhang, W., Wang, X., … Xia, F. (2017). Atmospheric volatile organic compounds in a typical urban area of beijing: Pollution characterization, health risk assessment and source apportionment. *Atmosphere*, *8*(3). https://doi.org/10.3390/atmos8030061

Zhang, Y., Li, R., Fu, H., Zhou, D., & Chen, J. (2018). Observation and analysis of atmospheric volatile organic compounds in a typical petrochemical area in Yangtze River Delta, China. *Journal of Environmental Sciences (China)*, *71*, 233–248. https://doi.org/10.1016/j.jes.2018.05.027